Dike Fields as Drivers and Witnesses of 20th Century Hydrosedimentary Changes in Highly Engineered Rivers

Gabrielle Seignemartin, Brice Mourier, Jérémie Riquier, Thierry Winiarski, Hervé Piégay

Dike fields as drivers and witnesses of 20th century hydrosedimentary changes in highly engineered rivers

G. Seignemartin[a, c], B. Mourier[a], J. Riquier[b], T. Winiarski[a], H. Piégay[c]

a. Univ. Lyon, Université Claude Bernard Lyon 1, CNRS, ENTPE, UMR5023 LEHNA, F-69518, Vaulx-en-Velin, France

b. Univ. Lyon, UJM - Saint-Étienne, CNRS, EVS UMR 5600, F-42023 Saint-Étienne, France

c. Univ. Lyon, ENS de Lyon, CNRS, UMR 5600 EVS, 69362 Lyon Cedex, France

Abstract

Many large European and American rivers have been channelized in the 19th century and since then feature Dike Fields (DFs) forming engineered alluvial margins. Drivers and witnesses of contemporary geomorphological and ecosystem changes, these initially aquatic DFs have for the most been filled with fine sediments and become terrestrial. On the Rhône River (France) which has not only been corrected but also equipped with numerous dams (mid-20th century), we studied the terrestrialization (*i.e.,* transformation of aquatic areas in terrestrial ones) in two types of DFs: open fields (groyne fields) and closed fields (groyne fields closed by a longitudinal dike). A classification of spatio-temporal terrestrialization patterns (5 types) has been obtained under GIS thanks to aerial photographs and completed by ground penetrating radar surveys to characterize the sediment structural organization of the deposits. It highlights local specificities (inherited forms) within a generalized trajectory of fluvial disconnection. Studying the evolution of the water lines and riverbed elevation allowed to emphasize the control factors and the associated forcings leading to terrestrialization. During phase 1 (reach only channelized – 1890s to 1970s), it is 47% of the closed fields areas which have been terrestrialized and 16% for open fields. Since the incision is not very pronounced on the reach, it appears to be mainly due to accretionary processes as a result of lower shear stresses within

the DFs. The terrestrialization from phase 2 (channelized and bypassed reach – 1970s-2000s) corresponds to 32% of the areas of closed fields and 51% of open fields. A cross-validation between the planimetric approach and a lateral connectivity model shows that dewatering caused by the flow diversion has provoked the emersion of almost the half of the DF extent on the upper – and most impacted – part of the reach (75% of the total terrestrialized area). In terms of fluvial rehabilitation, to understand the DFs trajectories provides new insights to guide future restoration design in line with the societal stakes and the current hydrological conditions. Strategical DF reconnections (removing or lowering dikes) could support the river to gain space and recreate hydrological connectivity gradients favorable to habitat diversity that it is currently unable to create or maintain on its own.

Key words:

river engineering; terrestrialization; groyne fields; floodplain; fine sedimentation; lateral connectivity.

1. Introduction

Over the past two centuries, the rivers and valleys from Europe and northern hemisphere have undergone an intensification of developments to maximise human control and benefits from fluvial systems. While some of the effects of the engineering developments were intentional and met the objectives of the time in which they were conceived, biophysical adjustments they triggered are now a management issue (Petts and Amoros, 1996; Gregory, 2006). Anthropogenic forcings have altered fundamental hydrologic and sedimentary processes that control eco-morphodynamic and have led to radical landscape and ecological changes (Petts, 1987; Dynesius and Nilsson, 1994; Nilsson and Berggren, 2000; Tockner and Stanford 2002; Gregory, 2006). As it is known that water-mediated exchanges (*e.g.,* sediment, organic matter, nutrients, organisms) and flood disturbances are key processes for habitat mosaic diversification and biodiversity (Geerling *et al.,* 2006; Amoros and Wade, 1996), hydrological disconnection (including longitudinal, lateral and vertical dimensions) is considered to be one of the main ecological alterations of river systems (Kondolf *et al.*, 2006; Amoros and Bornette, 2002; Ward, 1998)

Within this anthropo-complexity, certain infrastructures are widespread on engineered rivers. That is the case of channelization features, a common 19th century corrective intervention aiming to improve navigation conditions but also to gain floodplain space for human activities as well as increasing flood protection (Copeland, 1983; Brookes, 1985; Brooker, 1985; Sukhodolov *et al.*, 2002). Hydraulic infrastructures (classically groynes and longitudinal dikes) have been implanted "in" or "on the edge" of river channels to correct and fix its geometry on sinuous, braided, anabranching or meandering rivers (*e.g.,* Danube, Mississippi, Oder, Piave, Po, Rhine, Rhône). Also, in-channel structures directly limit lateral hydrological connectivity (Geerling *et al.,* 2006; Bravard *et al.,* 1986) and exacerbate overbank fine sedimentation on adjacent floodplain (Citterio and Piégay, 2009; Depret *et al.,* 2017). Dike fields (hereafter, DF) are no exception; they constitute sediment traps which partially or completely terrestrialized during the 20th century. Previous works have studied their impact on flow recirculation

(Copeland, 1983; Elawady *et al.,* 2001; McCoy, 2006; Papanicolaou and Fox, 2008), sediment deposition (Sukhodolov *et al.,* 2002; Schwartz and Kozerski, 2003; Savic *et al.,* 2013) as well as on ecological and geomorphological responses (Hudson *et al.* 2008; Buczyńska *et al.,* 2018). However, though these engineering structures are mostly present along highly developed reaches, factors controlling DF evolution from aquatic to terrestrial stages are not well explored notably in multi-pressure contexts: for instance, many of the channelized rivers were also developed for hydropower during the mid-20th century boom (Petts, 1984; Petts and Gurnell, 2005; Belletti *et al.,* 2020).

At the end, cumulative "natural" and anthropogenic forcings led gradually to the establishment of new terrestrial margins more or less ecologically functional – sometimes considered as impacted systems or novel ecosystem (according to Morse *et al.*,2014); but which are undoubtedly anthroposystems whose ecological interest must be assessed (Hobbs *et al.* 2006; Morse *et al.* 2014; Thorel *et al.*, 2018). To note that we would prefer the term terrestrialization (*i.e.,* transformation of aquatic areas in terrestrial ones) rather than sedimentation or deposition; aware that alluvial margin formation can be induced by sediment deposition and/or lowering of the water level due to different cascading adjusts.

In this context, identifying the factors controlling the DF evolution, quantifying their individual and combined effects is complex. That is why, in an original way on the dike fields, we propose to use a space for time substitution approach (Dépret *et al.,* 2017; Fryirs and Brierley*.,* 2012; Piégay and Schumm, 2003). The underlying strategy is to take into account local variability, while being able to detach from it in order to highlight the main controlling factors of the terrestrialization, and in particular, to understand the effect of the main engineering development phases. In the light of an interdisciplinary geohistorical study combining GIS approaches and Ground Penetrating Radar (GPR) surveys, the dike fields depict the entire 20th century fluvial disconnection trajectory, by being both drivers and witnesses of the developments and associated ecosystemic response. Also, while the restoration programs encourage to give back space to river (*e.g.*, with dike dismantling), it is crucial to be able to target the relevant levers and define a pertinent scale for functional rehabilitation so that

restoration action can be in adequacy with concrete environmental conditions while compromising with the societal stakes.

Our objectives are therefore to characterize (i) the terrestrialization trajectories within dike fields of a highly-regulated river, the Rhône River; (ii) the associate sediment patterns and deposits characteristics within the dike fields and (iii) identify and quantify the underlying processes and control factors.

2. Study area

The Rhône River is an 812km long river that originates in Switzerland at the Furka Glacier (2340 m asl) in the Swiss Alps (canton of Valais). Its watershed covers 98,500 km² of which 90,500 km² are located in France. It flows into the Mediterranean Sea with an average annual discharge of 1700 m^3/s at the Beaucaire gauging station located directly upstream from the delta (Olivier *et al.,* 2022). During the modern period, the Rhône was a multi-thread river. In many reaches, the river flowed in a fairly wide unvegetated gravel corridor, locally braiding or anabranching. After two last centuries development, the river mainly became a single-thread channel (Tena *et al.,* 2020; Riquier, 2015; Bravard, 2010).

We selected the Rhône River to explore such multi-driver contexts of groyne-field terrestrialization because its development history is complex. It can be sequenced in two main phases for which the effects of the developments can be studied. Phase 1 corresponds the 19^{th} century chenalization. Corrective hydraulic structures consist in classic groyne fields and – to resist high stream power of the river locally – in specific structures that are more robust. These ones are made up of transverse support dikes (called *tenons* in french). They are used as supports for submersible longitudinal dikes; forming the *Casiers Girardon* (named from the engineer who designed them). Phase 2 corresponds to the massive equipment of the river for hydroelectric production. It consists of 19 dams on the French part of the river that were built between 1948 et 1986 (except for the historical dam of Cusset built in 1898). Sixteen of them are bypassed schemes for which an artificial canal was built next to the river course and diverts

most of the bypass flow (management modalities depending on of each dam) supplying a hydropower plant (Annex 1). Following these two phases, the active channel has strongly incised and narrowed (Tena *et al.,* 2020; Parrot, 2015), side channels were disconnected (Dépret *et al.,* 2017; Riquier, 2015; Citterio *and* Piégay*.,* 2009) and corrective hydraulic structures were filled with fine sediments on which riparian vegetation developed (Räpple, 2018). Nowadays, the Rhône River is at the heart of rehabilitation projects and so the future of these alluvial margins – between conservation or dike removal – is questioned. Their ecological interest as possible novel ecosystems (Thorel *et al.,* 2018) – in particular that of riparian vegetation (Janssen *et al.,* 2020) – makes debate while a removal operation could be interesting to encourage a greater lateral mobility where it is feasible. Also, the inherited coarse sediments (corresponding to the former river bed below the fine sediment deposits) constitute an interesting alluvial stock for artificial gravel augmentation; to be promoted according to the risk of contamination represented by the overlying reservoir of fine sediments.

The studied reach is located in the Middle Rhône at the Péage-de-Roussillon section (PDR), which is one of the bypassed reaches of the river. It is 12.6 km-long and extends from the 50.6 River Kilometer (RK) to the 63 RK downstream of the city of Lyon (Figure 1.a & Figure 1.b).

This reach historically presented a braided pattern pursued then by a meandering style before the 19th and 20th century human interventions (Bravard *et al.*, 2008b). From the channelization development, it initially features 234 dike fields: 89 Girardon closed dike structures, 126 groyne fields, 19 other specific structures such as former side channel closing dikes (Räpple, 2018). Wide and long on average about 60 m by 130 m, they were cumulatively covering more than 108.2 hectares, with a density of 18.6 structures per river kilometer. In this study, we will only refer to classical groyne fields as “open fields”, the second ones as “closed fields” and both as “dike fields”. It will be considered that a dike field unit corresponds to the projected extent of the dikes which compose it (Figure 1.c). At PDR, the mean annual discharge is about 1050 m^3/s (Ternay gauging station) but since the diversion in 1977, only a minimal flow of 10 to 20 m^3/s runs through the bypass whereas most of the flow is diverted to a side canal for

hydroelectric production. The PDR hydroelectric plant capacity is overrun from 1600 m^3/s; in such case, the excess is released in the bypass. Conditioned by this threshold value, modalities of the floodplain hydrological connectivity are stretched between regulated low water conditions and severe erratic flood conditions. As per restoration plans, since 2014, the minimal flow has been increased to 50 and 125 m^3/s. Note that in 1979, a weir (*seuil de Peyraud*) was implemented in order to preserve some lands from water level modifications caused by the diversion.

Despite these heavy engineering developments, PDR remains a site of significant ecological value where many natural protection areas were established such as the National Nature Reserve of *la Platière* (1986), a Sensitive Natural Area zonation (1992), a Natura 2000 site (1992) and a Special Protection Area (Birds Directive, 2006).

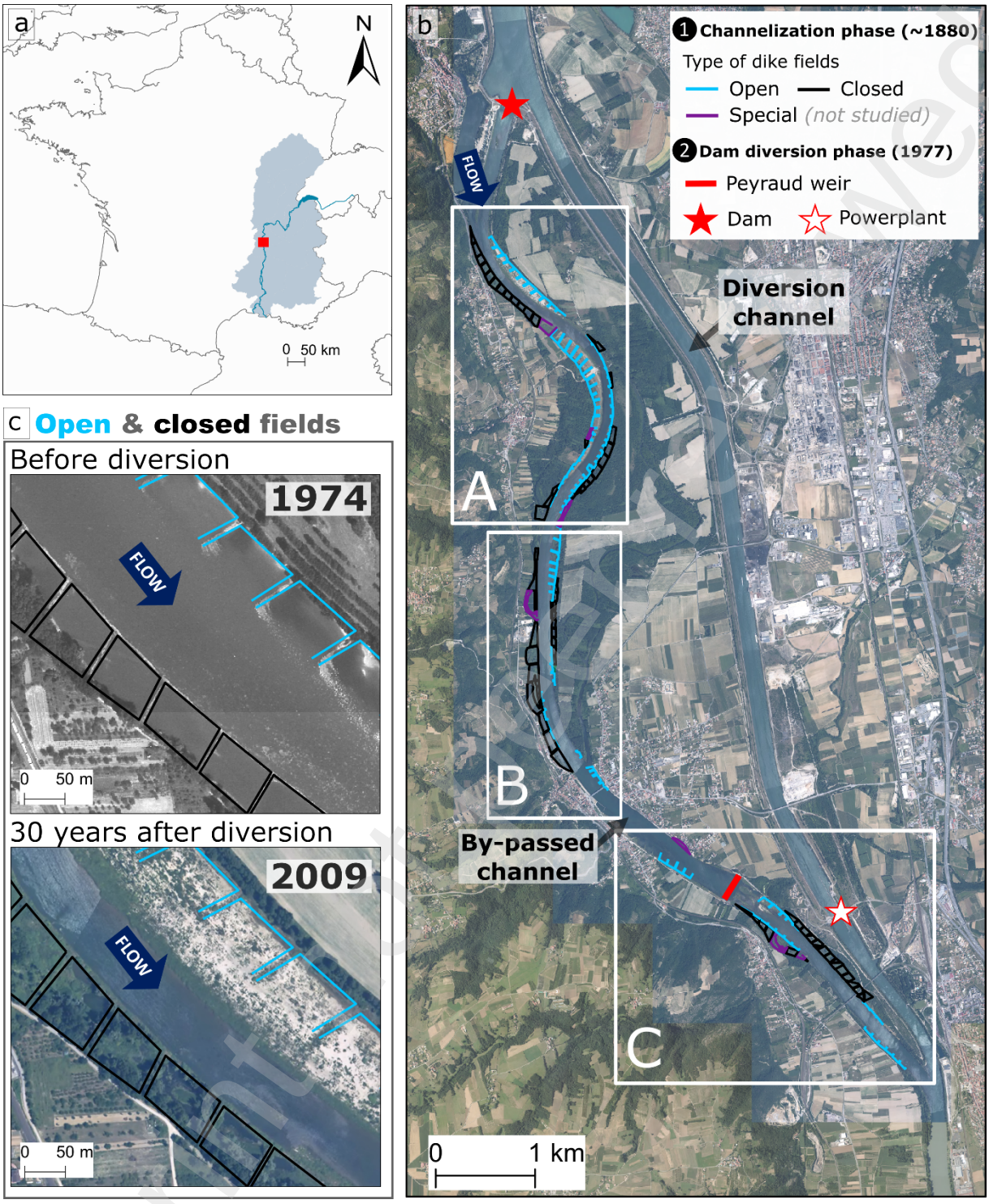

Figure 1 : a. Location of the Rhône River in France and of the studied reach: Péage-de-Roussillon (PDR); b. Overview of the dike fields (according to their type) in the bypassed reach of PDR and location of the sub-sectors corresponding to the analysis in Figure 4; b. Overview of open and closed field terrestrialization evolution before (1974) and 30 years after (2009) the diversion at PDR. Data source: Photography of 1974, IGN; orthophotography of 2009, BD ORTHO, IGN.

3. Material & method

To address terrestrialization, a GIS retrospective approach coupled with geophysics surveys was implemented to characterize the margin evolution and sediment deposits features. Inspired by theoretical and experimental sediment deposition patterns of Sukhodolov *et al.* (2002), we propose to rethink them with the GIS and historical data openings so that we obtain the diachronic perspective needed for any trajectory study. Regarding the drivers, the study strives to differentiate the processes underlying terrestrialization; notably with regard to the forcings linked to the water level lowering (incision versus flow diversion). To do this, we propose a multi-source approach using historical data (water line and river bed elevation) and overflow-driven lateral connectivity models (from Džubáková *et al.,* 2014).

3.1. Planimetric evolution of terrestrialization

Terrestrialization is first assessed by studying the planimetric evolution based on photograph archives georeferenced on GIS as it is now done classically (*e.g.,* Bryant and Gilvear, 1999; Winterbottom, 2000; Gilvear and Bryant, 2003). On the Rhône River, many studies have already used the available map and photographic archives to follow the evolution of the side channels and floodplains but do not focus on the dike field evolution (Riquier *et al.,* 2015; 2017; Dépret *et al.,* 2017; Tena *et al.,* 2020; Arnaud *et al.,* 2021).

3.1.1. Selection of aerial photograph series

The riverscape features were established under GIS (ArcMap™ 10.8) with georeferencing and vectorization processes of aerial images from the National Institute of Geographical and Forest Information data bank (IGN). Nine time series were selected in order to understand the role of each development phase on the terrestrialization processes (Figure 2). They are used to document the post-channelization / pre-diversion evolution of the beginning and the middle of the 20th century (1938, 1949, 1974), the direct impact of diversion (1979), the rapid post-diversion changes (1982 and 1986) and adjustments several decades after diversion (1991, 2002, 2009). Their scales vary between 1/15,000 and 1/25,000 for aerial photographs from

1938 to 2002. Orthophotographs from 2009 with a 66 cm pixel resolution served as a georeferencing base. All of their detailed characteristics (scale, acquisition technique, colour gradient, river discharge, etc.) are available in Annex 2.

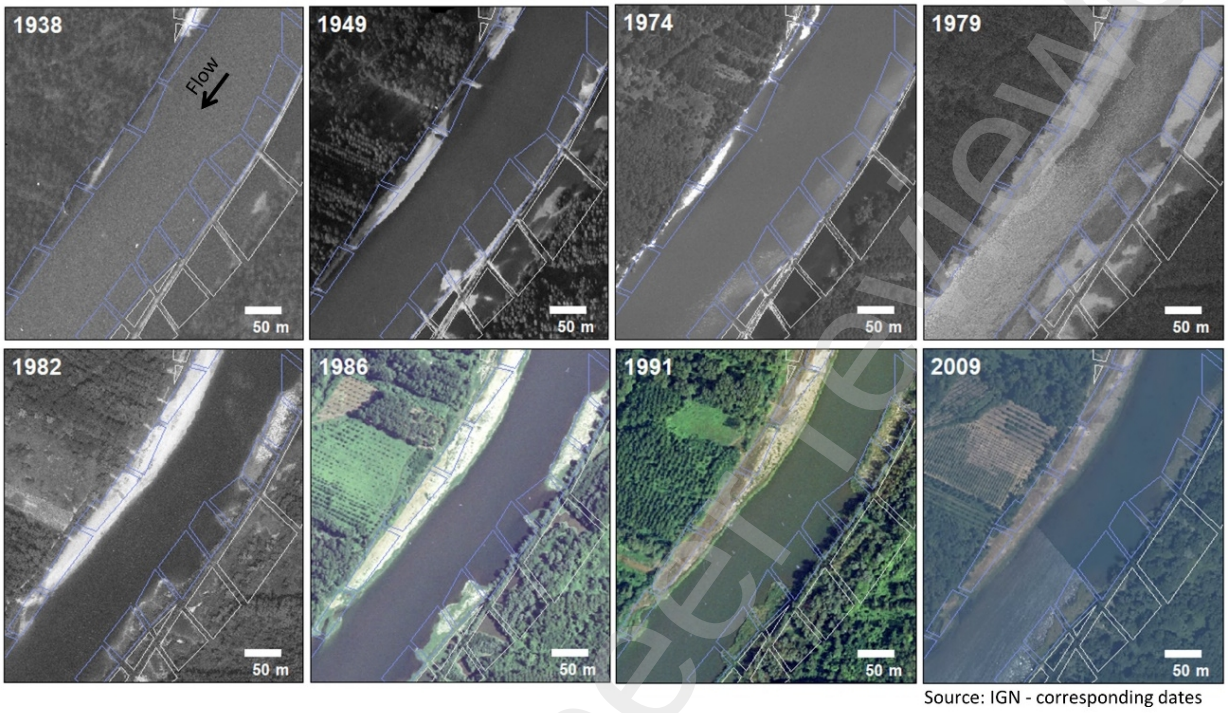

Figure 2: Diachronic photograph series from several dike fields located at RK 55.

3.1.2. GIS processing

The quality of fit on the DF scale was increased thanks to a specific georeferencing process in which the reach extent is divided by polygons of 2 kilometers long. Subparts of the photographs are georeferenced within these focusing areas all along the dike field succession (10 to 20 ground control points evenly distributed). As we concentrate on the DF evolution, dike crossings are used as ground control points as well as nearest infrastructures (bridges, buildings). The associated RMSE vary between 4.1 ± 1.6 m (1938 series) and 2.2 ± 0.9 m (2002 series), indicating that the associated rectification is fairly good-of-fit (*cf.* Gurnell, 1997; Arnaud *et al.,* 2015).

The limits between water and terrestrial areas were then digitized for each date with a scale ranging from 1:500 to 1:1,500 depending on the photograph quality. The photograph series that follow our selection give the information of the deposit stability and prevent from

interpretation errors due to the photograph quality variability. Also, the presence of woody riparian vegetation can make this limit unclear when their canopy overhang it. We drew them in an interpretative compromise of a few meters (2 to 10 m) from the edge of vegetation based on the scale relative indication of the existing breaks between tree crowns (Liébault and Piégay, 2002; Depret *et al.,* 2017; Tena *et al.,* 2020). Then, one polygon vector is created per photographs series, corresponding to terrestrial margin at each date. We also used an existing vectorial layer of the dike field implantation based on old maps and aerial photographs produced by Räpple (2018). By intersecting it with the multi-date polygon series, we obtain the in-dike diachronic evolution.

3.1.3. Quantitative and qualitative analysis of terrestrialization processes within the dike fields

Very specific dike configurations like half open dike fields (enough similar to wing groynes, *cf.* Przedwojski, 1995) were eliminated from the statistical planimetric study. Also, dike fields which are not directly located next to main channel and ones that display clear anthropogenic modifications (maintenance, engineering intervention, etc.) have been removed from the dataset. That is why we finally selected 193 DFs (85 closed fields and 108 open fields) on the 234 inventoried dike structures.

Cumulative Terrestrialized Areas (TA) were obtained by summing terrestrialized areas within the DFs over the entire sector according to the specified time window (Eq. 1).

$$\text{Cumulative TA} = \sum \text{mineral or vegetated surface within each dike field} \quad (1)$$

On the other hand, the evolutionary trajectories in terms of terrestrialization are examined depending on the percentages specific to each DF. For each date, the percentages of terrestrialization are obtained by the calculation (Eq. 2).

$$\text{TA}\,(\%) = \frac{\text{mineral or vegetated surface within the dike field}}{\text{extent of the dike field}} \times 100 \quad (2)$$

Inspired by the inter-groyne deposition patterns of Sukhodolov *et al.* (2002), the terrestrialization pattern classification is determined with an empirical and expert methodology based on the observation of the planimetric recurrences but also on the evolutionary aspect thanks to the multi-date dataset.

3.2. Characterization of fine sediment deposits within the dike fields

We combined telemetric and geophysical datasets to assess the organization of fine sediment deposits and link it with the planimetric history. Each approach aims to cover different features and scales. We characterise the topography of the alluvial margins (reach scale) using a LiDAR DEM. A GIS model based on the study of fine sediment thickness allows us to better assess the sediment storage within dike fields on two third of the reach length. Subsurface profiles obtained by Ground Penetrating Radar provide information on sedimentary structures within the DFs.

3.2.1. Topographic dataset

For the elevation dataset, we use an airborne LiDAR Digital Elevation Model (DEM) produced in 2010 by the IGN. It has a 2 m resolution and a 0.2 m vertical accuracy. The pulses density is of 1 to 2 per square metre for which a pulse is a 0.4 m diameter disc (IGN, 2010). For each DF, the average elevation was calculated from this DEM on the total extent. For the elevation associated to chronoplanimetric time window, it is calculated on the associate extent within the DFs. The topographic transect were extracted from the LiDAR DEM thanks to the 3D Spatial Analyst tool from ArcMap™ 10.8.

3.2.2. Gravel layer GIS model based on metal rod probing

The dike fields trapped fine sediments that deposited on a layer of coarse sediments (gravel and pebbles; hereafter, gravel layer). Thus, the limit between coarse sediments and fine sediments embodied by the gravel layer not only constitutes a chronological marker but physical evidence of the geomorphological process modifications of the Rhône. To estimate its delimitation, more than 330 sampling points were surveyed between the RK 52 to 58. The

depth to gravel - and so the fine sediment thickness of the sub-deposit - was estimated by driving a 1 cm diameter metal rod into the fine sediment deposit until it hits the gravel layer (Tena *et al.,* 2020; Piégay *et al.,* 2008; Dufour *et al.,* 2007). Using this dataset, the gravel layer and fine sediment thicknesses were modelled using a GIS cokriging method (Piégay *et al*., 2015). From this dataset, fine sediment thicknesses within the DFs were extracted according to each date of the planimetric history.

3.2.3. Ground penetrating radar subsurface images of the sediment deposits

The characterisation of the sediment structure was investigated by Ground Penetrating Radar (GPR). It is a non-invasive geophysical method based on a principle of high frequency electromagnetic energy signal reflection. It provides high resolution images of shallow subsurface structures and is often used in sedimentological studies (Davis and Annan, 1989; Beres and Haeni, 1991; Gawthorpe *et al.,* 1993).

We use a GSSI SIR 3000 structure (Geophysical Survey Structure Inc., Salem, USA), with a shielded antenna at a central frequency of 200 MHz in monostatic mode. The compilation and the juxtaposition of the signals recorded during the movement of the radar antenna make it possible to obtain a vertical profile (*i.e.*, radargram). On radargrams, the reflectors correspond to the reflection lines of the signal associated with changes in the ground structure and/or texture. It shows the main sedimentary structures and their interpretation gives an idea of the deposit organization (Vauclin, 2020; Regli *et al.,* 2002; Beres *et al.,* 1999).

Three transects running on 380 m were carried out to provide a representative panel of deposit structures according to the chronoplanimetry and DF type (open/closed). Transect GPR T1 long of 100 m is oriented West to East and crosses transversally a closed field in a concavity of the left bank (RK 54.625). Transect GPR T2 (d = 140 m) is oriented North to South, parallel to the channel and crosses 3 closed fields lower in the same concavity (RK 55.1). Transect GPR T3 (d = 140 m) is also oriented parallelly to the channel and crosses 3 open fields in a convexity of the right bank (RK 54.1).

3.3. Assessment of terrestrialization due to channel incision

If sedimentary deposition surely contributes to terrestrialization, different hydro-geomorphic processes such as river bed incision or flow diversion can cause a lowering of the water level and also lead to terrestrialization. So, we aim to apprehend the incision phenomenon by monitoring the vertical evolution of the river bed. By monitoring the evolution of the water lines, it is possible to assess the effect of the incision on it (at comparable discharge states) and the impact of the dewatering that followed the diversion flow (total versus residual discharge).

3.3.1. River bed evolution during the 20th century

River bed elevation and in particular incision phenomenon have been studied by Parrot (2015) according to three periods. She established (i) a reference state in 1897, (ii) a "post-channelization – recently diverted" state (1982) and (iii) a current "post-channelization – post-diversion" state (2008). They were extracted from bathymetric transects collected every 500 m at sus-mentioned dates (Topographic Data Base of the Rhône; IGN, 2010).

3.3.2. Water line evolution during the 20th century

To enlighten the early 20th century situation while the channelization has just been realized, we used a 1902 elevation dataset of the water line (WL) at low flow that is known for each RK (from *Fascicule Armand des pentes du Rhône*, 1902). For the post-channelization and pre-diversion WL characterization, two surveys of the waterline made by the *Compagnie Nationale du Rhône* (CNR) were available for the post-chenalization/pre-diversion situation (1962) at low flow (260 m^3/s) and mean annual flow (1080 m^3/s). The first one was used as a comparison to 1902 situation and the second one as a reference of average conditions at this time (1080 m^3/s). For the recent post-diversion situation, the 2010 WL elevation was available in the BDT Rhône. It corresponds to the minimal flow in the bypassed reach (20 m^3/s). The states they informed, the comparisons and insights they allow are summarized in table 1.

312 Table 1: Available data set about the water line evolution on the PDR reach during the 20th century
313

Date	Source	Development state	Discharge indications	Informed state	Comparisons and insights
1902	*Fascicule Armand des pentes du Rhône*	Just after channelization	Low water	Reference state at the beginning of the 20th century	Channelization effect on water line NB: similar discharge conditions
1962	CNR	60 years after channelization, before flow diversion	Low water (260 m^3/s)	Reference state at low flow conditions at the end of phase 1	
1962	CNR	60 years after channelization, before flow diversion	"Normal" discharge (1080 m^3/s)	Reference state in average conditions at the end of phase 1	Flow diversion impact on water line in a channelized situation (cumulative impact) NB: discharge conditions are different but representative of the average conditions of each phase
2010	BDT Rhône	More than 100 years after channelization 31 years after flow diversion	Minimum flow Residual discharge (20 m^3/s)	State in average conditions at the end of phase 2	

314

315 *3.3.3. Dike field relative elevation and change in water line position*

316 If the water lines change, so does the channel-DF relationship. To evaluate this evolution, we
317 use a relative elevation (RE) indicator from the DFs to the water line. The dike field RE to the
318 WL is obtained according to the following calculation (Eq.3):

319 $$\text{Dike field RE (m)} = \frac{\text{dike field elevation averaged on its total extent}}{\text{water line elevation in the cross section}} \quad (3)$$

320 The delta between 1962 (pre-diversion) and 2010 (post-diversion) WL situation constitutes an
321 indicator of connection changes between the active channel and the alluvial margins. For lack
322 of a 1962 DEM Lidar, the 1962 dike field relative elevation to water line is also based on the
323 2010 dike field average elevation. Thus, it is a partial disconnection indicator because it is only
324 focused on the WL changes and does not include overbank sedimentation effect that would
325 be taken into account if we would have a DEM for the pre-diversion state.

326 ## 3.4. Assessment of terrestrialization due to water diversion

327 In order to address the contribution of diversion dewatering in terrestrialization, we aimed to
328 model the submerged surfaces corresponding to a projected active channel in discharge
329 conditions relative to situation before and after flow diversion. To do this, we use models of

overflow-driven lateral connectivity developed by Džubáková *et al.* (2015). They also served the purpose of making the link between residual hydrological connectivity and the up-to-date state of terrestrialization.

3.4.1. Overflow-driven lateral connectivity models and by-products

The hydrological connectivity of alluvial margins was approximated thanks to the overflow-driven lateral connectivity model raster from Džubáková *et al.* (2015). It was developed in MATLAB and C ++ environments involving the sus-mentioned DEM LiDAR (2010), rating curves and flow time series (daily discharge over the 1986-2010 period). Rating curves are used to obtain water levels associated with water discharge. These levels are then projected onto the floodplain by assuming that the water level is homogeneous within the cross section and decreases in the downstream direction. Based on that principle, a model of overflow-driven lateral connectivity was obtained with different attributes: pixel submersion frequency (days/year), critical discharge leading to the pixel submersion, etc. The model developed on the PDR reach only extends from RK 52.5 to RK 60.

3.4.2. Active channel area based on the modelled critical discharge for submersion

We used the model of "critical discharge for pixel submersion" to obtain estimations of the area submerged in conditions that are representative of the average conditions of each development phase (total versus minimal flow). Thereby, we compared the flooding areas for a discharge corresponding to 1050 m^3/s (mean annual discharge at the nearest gauging station) and to 20 m^3/s (residual discharge during the 1977-2014 period). The difference between the two extents highlights the effect of the dewatering induced by diversion.

We also used the 2010 DEM LiDAR to model the submerged area corresponding to 1050 m^3/s (*i.e.,* total discharge) because we had no DEM for the pre-diversion reference state. Because the 2010 DEM LiDAR represents the topography including post-diversion sediment deposited, the model could overvalue the water volumes. By this way, it could overestimate the flooding

area associated to a 1050 m^3/s discharge in pre-diversion situation (with less sediment deposited than on the 2010 situation).

3.4.3. Link between current terrestrialization rate and hydrological connectivity of the DFs

The link between the average flooding frequency of the DFs (hydrological connectivity proxy) and the terrestrialization rate of the DFs was assessed by a Generalized Linear Model (GLMs). Because the percentage of terrestrialized area is a proportion and the flooding indicator a frequency, we used a binomial function link. Employing the glm function of R (version 4.0.3), we detailed the proportion of deviance explained (D^2) that we obtained by using the Dsquared function of the modEvA package. The model is performed on a dataset of 116 dike fields corresponding to the extent of the submersion frequency raster which covers two thirds of the reach (from the dam to the Peyraud weir; *cf.* Figure 1).

4. Results

4.1. Terrestrialization processes in space and time

4.1.1. Cumulative terrestrialized area

The quantitative approach reveals that the cumulated closed field extents cover 38.87 ha of which 47% (18.31 ha) have been terrestrialized during the pre-derivation period, 32% (12.53 ha) during the post-derivation period whereas 21% (8.03 ha) of their surface remain aquatic. In open structures that cover 39.3 ha, 16% (6.18 ha) correspond to surfaces terrestrialized during the pre-derivation period, 51% (20 ha) during the post-derivation period whereas 33% (13.12 ha) of their surface have remained aquatic.

The general trend towards terrestrialization of alluvial margins including differences in the temporal sequences between the two types of dike fields is highlighted in Figure 3. During phase 1, the phenomenon is already underway in the closed fields while it is very little in the open fields. Indeed, the average percentage of terrestrialized areas (TA) in closed fields reached 26.9% in 1938, *i.e.*, 40 years after their establishment. Between 1938 and 1949, TA

increased to 40.4%. Between 1949 and 1979, the phenomenon slowed down: in thirty years, the average TA only increased by 7%. Regarding open dike fields, only 5.9% of their surfaces were terrestrialized in 1938. The average percentage increases to 11.4% and stagnated during the 1949-1979 period.

During the second phase, the terrestrialization phenomenon gets carried away. In the closed fields, over the period 1979-1982, the average TA had considerably increased from 49.3% to 67.9%. After this strong acceleration, terrestrialization slowed down again and the TA stagnated around an average of 81%. In open fields, the average percentage of TA has been multiplied by 4.1 over just a few years going from 12% to 49%. Then, it had stalled around 52% during the 1991-2009 period.

These general trends to terrestrialization are accompanied by significant variability due to the specific trajectories of the different types of dike fields. For the closed fields, the interquartile ranges (IQR) of the TA percentages are homogeneous (from 1938 to 1986: IQR ranging from 30.5 to 42.8) even if it is possible to note that it decreases between 1986 and 1991 (IQR_{1986}=39.3; IQR_{1991}=31) then stagnates on the later dates (IQR_{2002}=28.2, IQR_{2009}=28.3). For open fields, the opposite trend is observed. Mainly aquatic before diversion, the interquartile deviations are firstly stretched during the phase 1 (from 1938 to 1979: IQR ranging from 6 to 23). After the diversion, the associated IQRs become very pronounced covering at the maximum in 1986 92.4 % of the spectrum and reflecting the variability of open field configurations. We also note that there are many more outliers with higher percentages of TA before diversion for open fields, while the opposite situation is reported in closed fields with fewer outliers characterized by lower TA percentages.

4.1.2. Terrestrialization space-time patterns

The chronoplanimetric analysis clearly show the formation of alluvial margins and the role of each engineering development phase. The maps (Figure 4) provide an overview but also insight into more local trends in the terrestrialization history.

Older pre-diversion terrestrialized areas (dark green to light green surfaces) are mostly located at the back of the closed field. Post-diversion areas (warm colors corresponding to “after

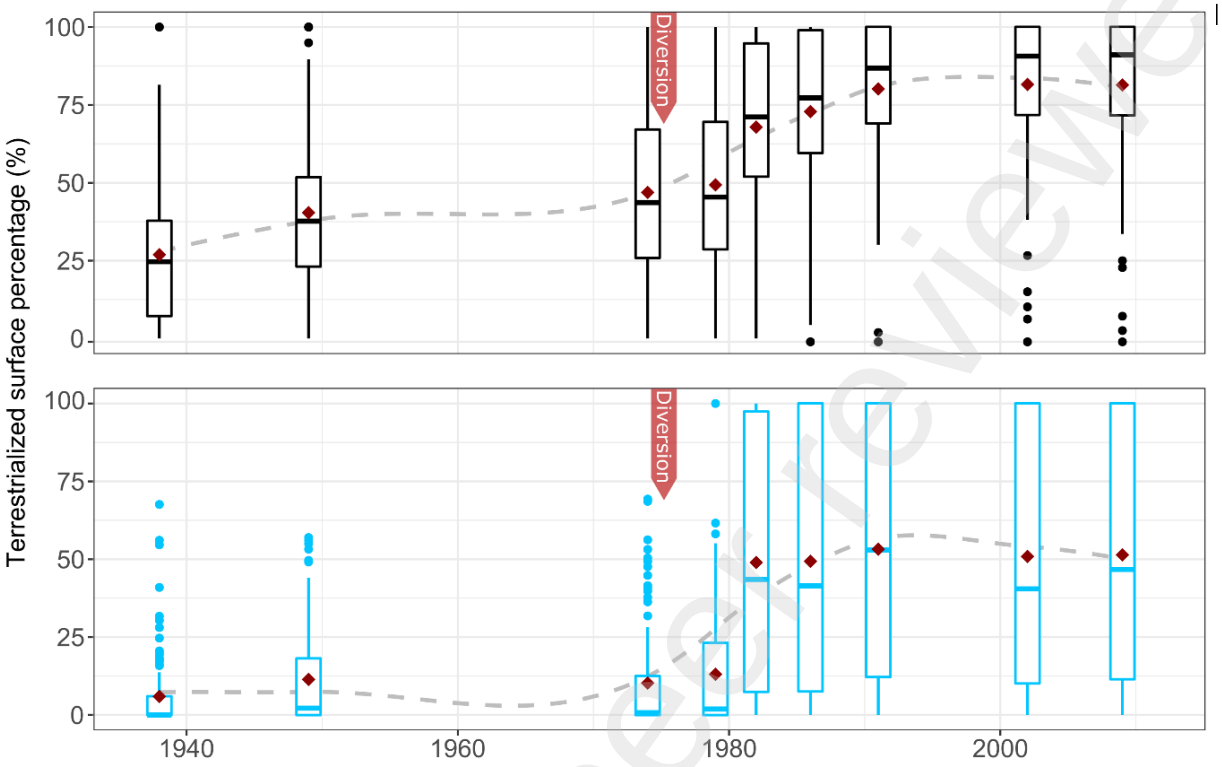

Figure 3: Terrestrialization percentage evolution within the dike field extents throughout the 20th century ($n_{closed\ fields}$ = 85, $n_{open\ fields}$ = 108 where closed fields are in black and open fields in blue; red symbols correspond to the averages)

The Figure 4.a shows the planimetric evolution at the scale of a meander. In concavity (right bank), some closed fields have gradually terrestrialized, which results in shades of green (pre-diversion terrestrialization) in the back of the structures whereas warm color surfaces are leaning against them (post-diversion terrestrialization). On the left bank, within the channel convexity, there are unicolored open fields (light orange corresponding to 1979-1982-time window) which therefore terrestrialized uniformly and quickly after the diversion.

The Figure 4.b depicts the situation upstream of the Peyraud weir. It is first characterized by a straight which ends on a meander corresponding to the bend of two-thirds of the bypassed reach. On the right bank, many closed fields have been implanted at the level of and former side channel and its associated island (*île de Poucharle*). They are marked by first phase

terrestrialized areas and remaining aquatic surfaces. On the other hand, the closed fields located in the heat of the concavity are still entirely aquatic. On the left bank, the planimetric dynamics are different depending on local conditions: the open fields located in the convexity upstream of the sub-sector have been partially terrestrialized mainly in phase 2. The southernmost open fields, which are smaller and in a straight section have not been terrestrialized. Closed fields that benefit from the open field protection began to strongly terrestrialize from phase 1 while the others do so more during phase 2.

The Figure 4.c displays the situation in the straight section located downstream of the Peyraud weir. On the right bank, in the first row, there are open fields still aquatic. Behind these, closed fields have been built to close a former side channel and are surrounding the associated island. Around this island, the surfaces have mainly terrestrialized during the first phase (green colors). On the left bank, there is a series of open fields that have been more or less terrestrialized during phase 2. The two closed fields protected by a first row of open fields were mainly terrestrialized during phase 1, while the following ones – directly exposed to the channel – were terrestrialized more gradually, with numerous post-diversion patches or still aquatic areas.

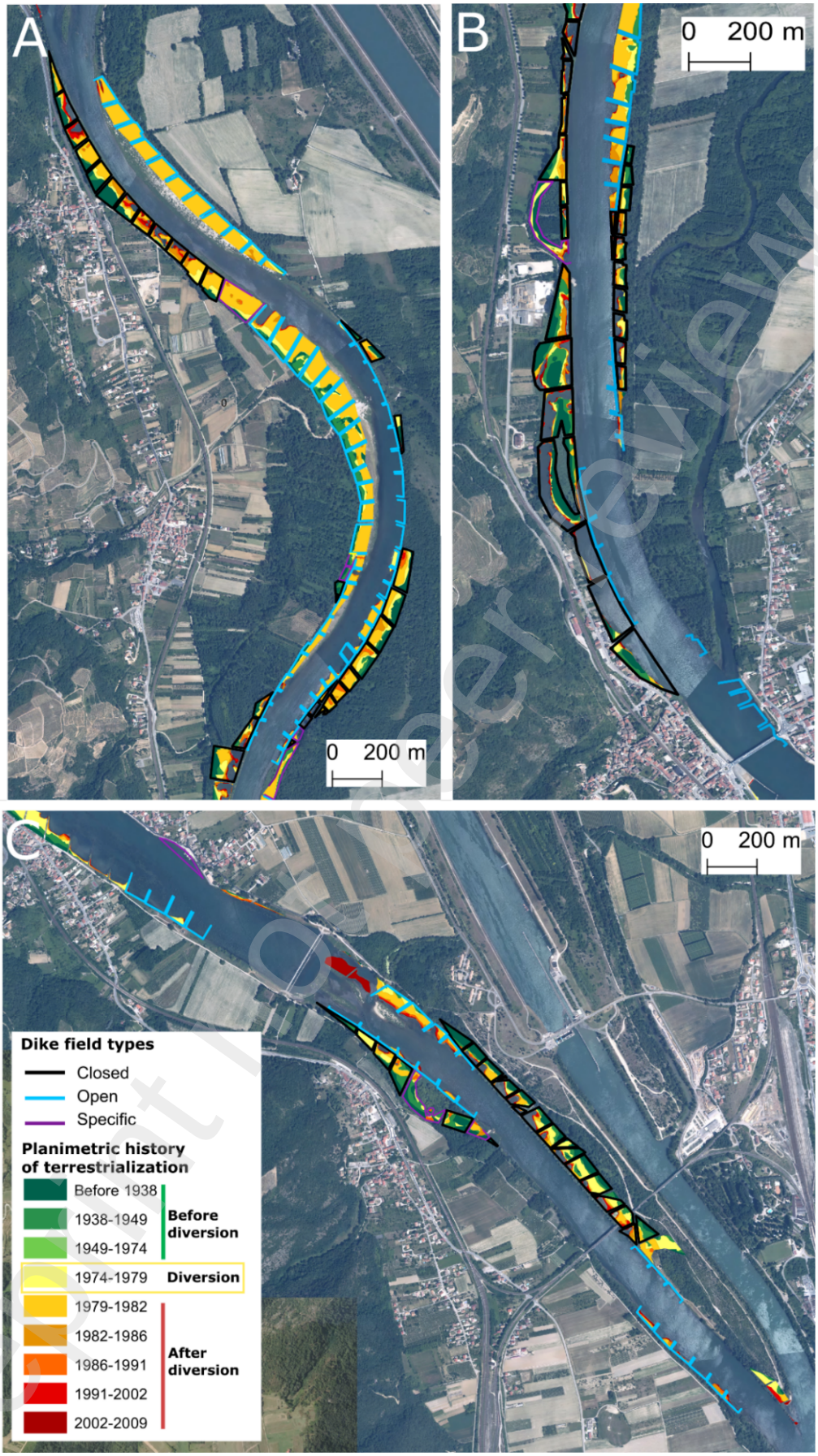

Figure 4: Planimetric patterns of terrestrialization through time within the dike fields of the Péage-de-Roussillon bypassed reach during the 20th century. Sub-sectors a, b and c are localized on Figure 1. (Data source: orthophotography of 2009, BD ORTHO, IGN; planimetric vectors from the dataset presented in section 3.1).

4.2. Chrono-planimetric recurrences and classification of terrestrialization patterns

Although differences were observed according to local conditions and the type of DFs, the chrono-planimetry show many recurrences (Figures 3 and 4). Depending on the prevalence of observed forms, associated periods of terrestrialization and structuring similarities or singularities, five categories of terrestrialization patterns were defined: aquatic, lateral, concentric, after dam strip and complex (Figure 5). The aquatic type is associated with a DF surface that remains unterrestrialized for more than 85% of the DF extent (limit based on natural distribution breaks). Lateral type is characterized by a partially or totally terrestrialized area with multiple successive terrestrialized bands of varying sizes and distributed laterally to the bank or angularly to the transversal dikes. Concentric type is characterized by being highly terrestrialized (~10% of remaining aquatic areas) and the presence of areas with progressive concentric closures that may remain aquatic or end up by gradually terrestrializing. After-dam uniform patterns correspond to uniform patches that terrestrialized consecutively to the diversion (light orange corresponding to 1979-1982 after diversion time window). For the complex group, the DF surface is more or less terrestrialized and shaped according complex forms caused by geomorphological specificities (*e.g.,* presence of former side channels, old islands).

Regarding the percentage of terrestrialization, TA% are significantly different (p-value = $4.04E10^{-6}$) reaching 81.4 ± 24.5% for closed fields and 51.39 ± 40 % for open fields (Table 2). Out of a total of 85 closed fields, we identified only 2 aquatic patterns (associated TA%: 4.9 ± 3.3%), 18 that are lateral (TA%: 66.1 ± 31.8%), 41 that are concentric (TA%: 85.1 ± 12.8%), 7 are after-dam uniform ones (TA%: 100%), 11 are complex ones (TA%: 84.6 ± 23.45%) (Table 2). Also, 6 closed fields are classified as “already full” which are dike fields with an early filling – at the beginning of the 20^{th} century – for which the absence of information makes it irrelevant to associate them with a pattern. From the first photo archive (1938), they are already strongly or entirely terrestrialized.

Out of a total of 108 open fields (Table 2), we identified 22 aquatic patterns (associated TA%: 3.2 ± 5.2 %), 49 are lateral (TA%: 50.4 ± 25.3), 3 are concentric ones (TA%: 89.6 ± 10.7%), 20 are after-dam uniform ones (TA%: 96.2 ± 17%) and 14 are complex (TA%: 85.3 ± 26.2%). Thus, aquatic patterns are mainly observed in open fields, lateral ones in both types of DFs, concentric ones mainly in closed fields, after-dam uniforms in both but mainly in open fields. Finally, the complex patterns which transcribe local specificities are associated with two types of DFs whose implantation was itself a function of local conditions.

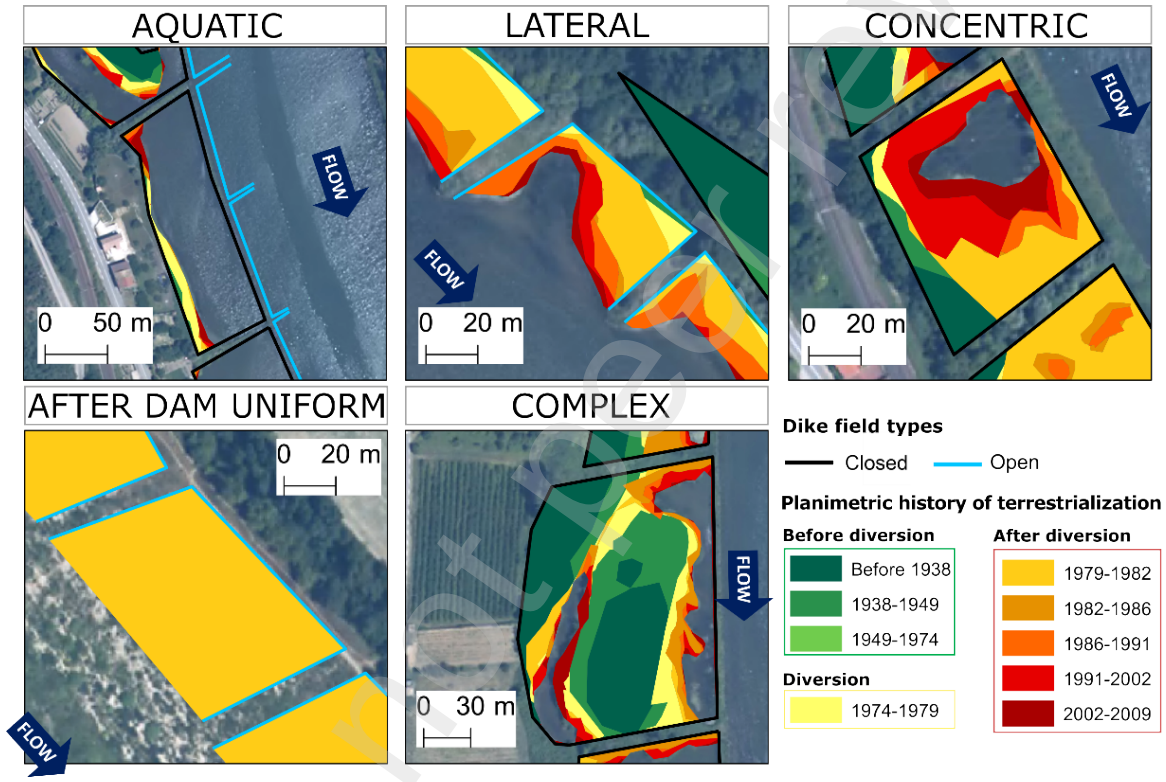

Figure 5: Classification of recurrent terrestrialization patterns (Data source: orthophotography of 2009, BD ORTHO, IGN.

Table 2: Pattern occurrences and associated percentages of Terrestrialized Area (TA%) in closed and open fields.

	Pattern type	Aquatic	Lateral	Concentric	After dam uniform	Complex	Already full	Total
Closed fields	**Count (*n*)**	2	18	41	7	11	6	85
	TA% (Average ± SD)	4,9 ± 3.3	66.1 ± 31.8	85.1 ± 12.8	100	84.6 ± 23.5	100	81.4 ± 24.5
Open fields	**Count (n)**	30	41	3	20	14	x	108
	TA% (Average ± SD)	3.2 ± 5.2	50.4 ± 25.3	89.6 ± 10.7	96.2 ± 17	85.3 ± 26.2	x	51.39 ± 40

4.3. Architecture of sedimentary deposits in relation to terrestrialization patterns

The architecture of the sedimentary deposits was approached by geophysical surveys to corroborate their geohistory and better understand the vertical pattern. On the radargrams (GPR outcomes), feature delimitations are drawn by the variation of the reflectors caused by the changes in texture and density. It is then possible to identify structuring elements such as the dikes or the gravel layer corresponding to the old river bed made up of coarse alluvium (Figure 6). Above the thick reflector interpreted as top of the gravel layer, we observe different structures, with more or less marked reflectors depending on the transects that we wanted to be a representative panel of deposit structures according to the chronoplanimetry and DF type (open/closed).

The GPR T1 transect is transverse. It crosses a closed field with a transversal pattern (CF1) and extends over the alluvial floodplain. Between 3 and 4 m, there is a feature corresponding to the longitudinal dike d1. Between 20 and 50 m, the reflectors located below the one highlighted in yellow are thicker and present more or less parallel reflectors with sigmoid patterns. The surface vector refers to the chronoplanimetry that can be observed on the associated map: the levee located between 37 and 42 m is concordant with the change between the pre and post-derivation period. The formerly terrestrialized surfaces (before 1938) are higher than the recent ones (+2.8 to 3.5m).

The GPR T2 transect runs along the longitudinal dike of closed fields (CF2, CF3 and CF4) located in two dike fields further downstream from the GPR T1. It crosses d2 and d3, two lateral transverse support dikes. The radarfacies are generally less contrasted than those of the GPR T1, in particular behind the d2 and d3 dikes corresponding to fine sediment pools (between 50 to 70 m and 115 to 140 m). Thicker sediments are observed under the reflector highlighted in yellow between 70 and 110 m. All the chronoplanimetry of the transect corresponds to post-derivation time windows. The fine sediment pools are associated with the period 1986-1991. Topographically, there is little variability except at the level of the pool depression (about 1 m).

The GPR T3 transect covers open fields (OF1, OF2 and OF3) longitudinally to the channel in an area mainly terrestrialized following the diversion (1979-1982). It crosses two groynes noted g1 and g2. The reflectors here are much more contrasted and depict coarser alluviums than in the closed fields. Between 0 and 38 m, the reflectors are rather parallel and thick until meeting g1. After g1, there is a depression between 42 and 58 m which gradually reduced in direction of g2. The reflectors are firstly thick and become thinner as we get closer to g2. Behind g2, there is the beginning of another depression marked there also by underlying deposits with very thick reflectors. Topographically, the variability is moderate on the T3 transect (delta of 2 m).

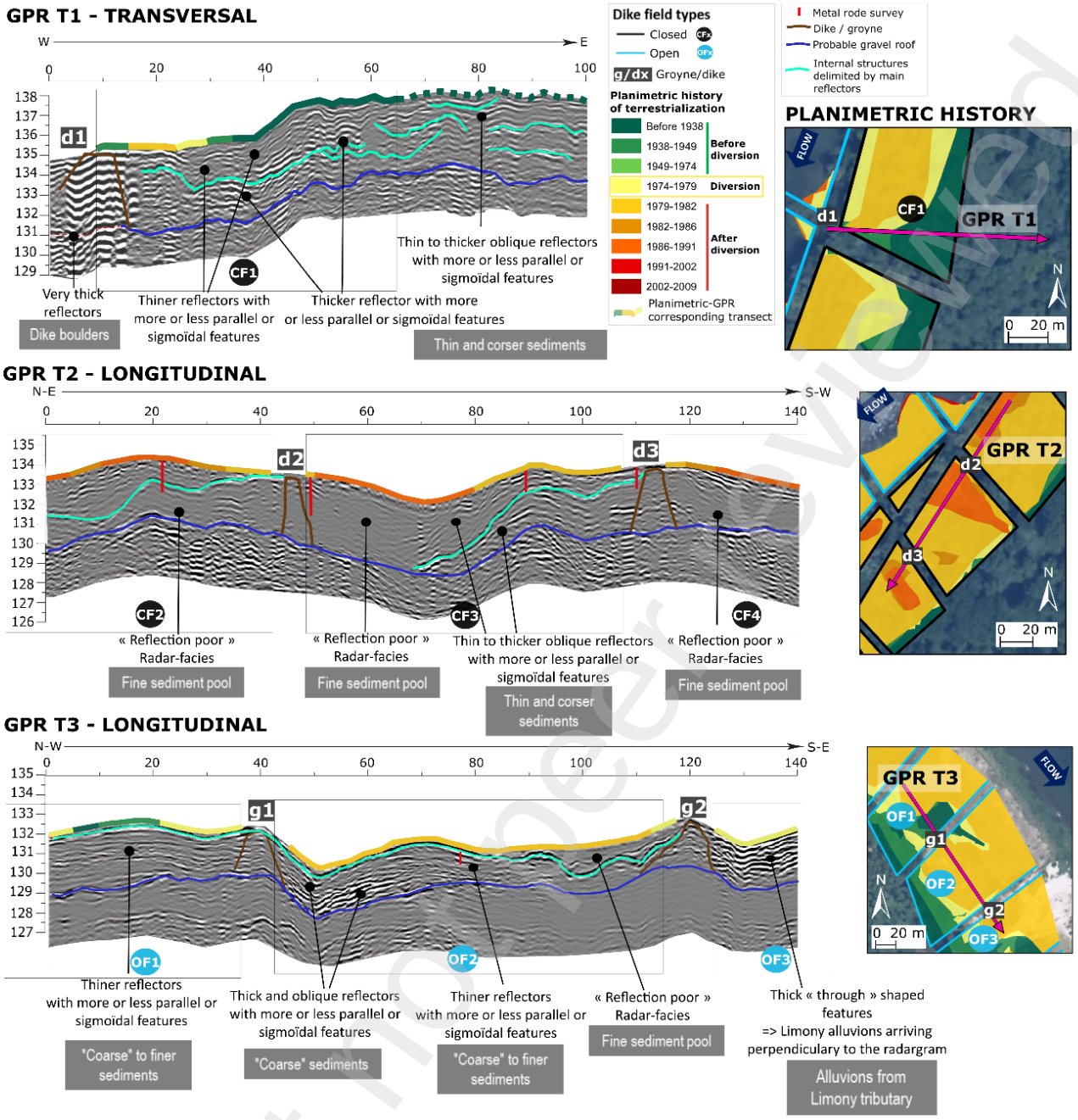

Figure 6: Ground Penetrating Radar survey of 3 transects crossing some closed fields (GPR T1 and GPR T2) and some open fields (GPR T3) and their associated planimetric history at PDR. (Data source: orthophotography of 2009, BD ORTHO, IGN; planimetric vectors from the dataset presented in section 3.1).

Data of topographic variability and fine sediment thicknesses - according to the periods of terrestrialization - were extracted from the LiDAR DEM and the thicknesses raster (Figure 7). The average elevation and fine sediment thickness values associated with each chronoplanimetric sequence were calculated within the dike fields (n_{DF} = 135) on the available dataset between RK 52 to 58. The elevations specific to the chronoplanimetric sequences

show a marked gradient (*cf.* Figure 7.a; Kruskal-Wallis, p-value < 2.2e-16) with higher elevations for the oldest sequences (maximum observed before 1938 = 3.63 ± 1 m) and lower elevations for the most recent sequences (maximum observed for 2002-2009 = 0.68 ± 0.3 m). The alluvial margins are stepped according to their geohistory with very distinctive limits (*cf.* Figure 7.b; Kruskal-Wallis, p-value < 2.2e-16). Also, all the Wilcoxon tests show significant difference of elevation except for the last three chronoplanimetric sequences that are more homogeneous. The example of topographic cross-section (Figure 7.c) illustrates topographic variability according to the period of terrestrialization and highlights a levee at the pre/post-diversion limit of the chronoplanimetric sequences (at 90 m). Greater thicknesses are observed with chronoplanimetric sequences from the beginning of the 20th century (max before 1938 = 2.21 ± 1.1 m) compared to more recent ones (min for 2002-2009 sequence = 0.91 ± 0.64 m). However, the 1982-1986 sequence stands out, with significantly greater thicknesses than other post-diversion chronoplanimetric sequences (1.36 ± 0.7m; *cf.* Wilcoxon tests on Figure 7.b).

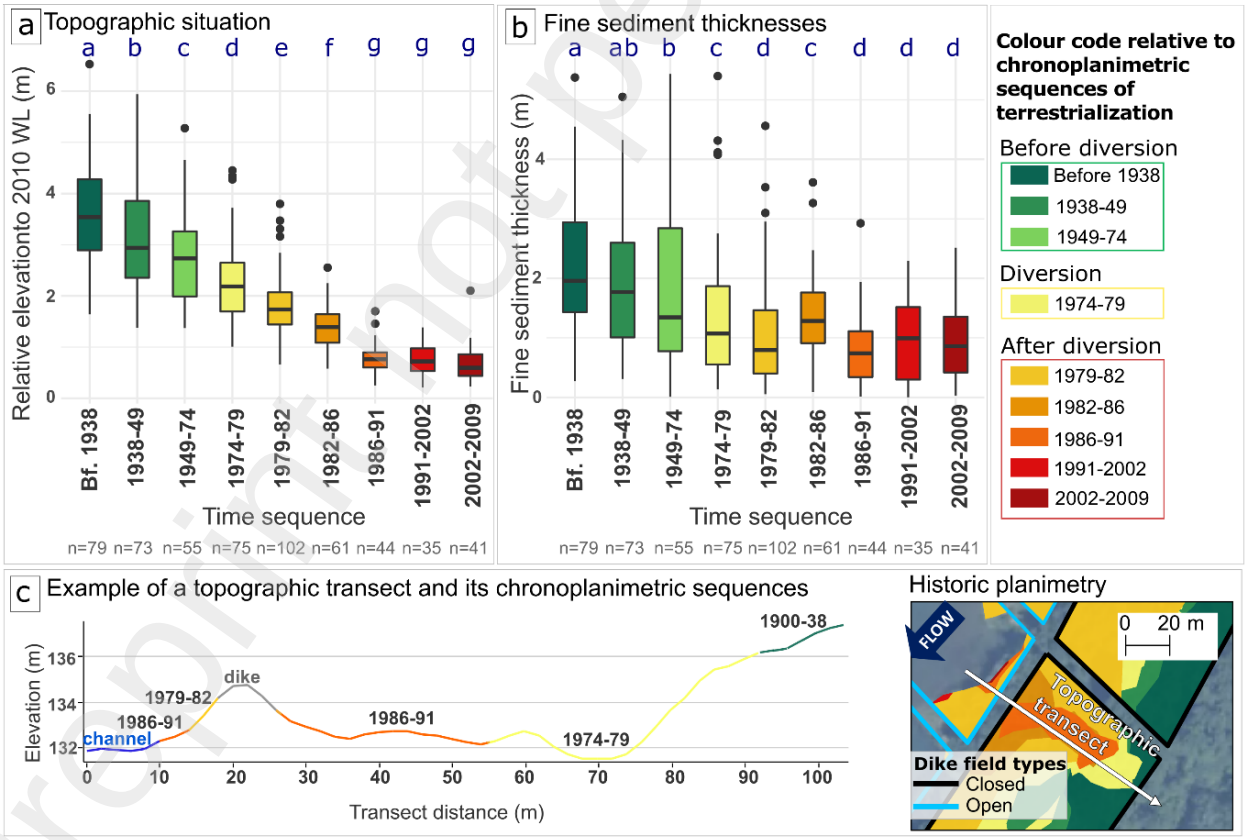

Figure 7: a. Topographic situation of the sediment deposits to the 2010 water line according to their terrestrialization history at PDR. Wilcoxon tests were performed and significant differences (p-value <0.05) are specified according to the letter classification; b. Fine sediment thicknesses based on

calculations from the MNT Lidar dataset and the gravel roof model at PDR. Wilcoxon tests were performed and significant differences (p-value <0.05) are specified according to the letter classification; c. an example of a transversal transect crossing an open and a closed field at PDR, its associated historic planimetry allowing the observance of before-after diversion heterogeneity. (Data source: orthophotography of 2009, BD ORTHO, IGN; planimetric vectors from the dataset presented in section 3.1). River bed and water line elevations changes caused by engineering developments and associated DF disconnection

4.3.1. Phase 1: channelized situation (1900s-1970s)

On the sub-sector between RK 52 and 63, an average river bed incision of -0.92 m is observed on phase 1 with a maximum of -3.41 m at RK 59 (Figure 8.a). A maximum bed incision of -5.64 m is observed at RK 63.5, downstream of the studied sub-sector.

The 1902 and 1962 WL at low water evolve according to a regular upstream-downstream gradient. They present rather equivalent slopes even if that of 1962 is slightly more pronounced (1902 WL Slope: 0.0443% and 1962 WL Slope: 0.0475%). The 1962WL at low water is lower than 1902 one, on average by -1.07m with local variations between -0,62 m (RK 50) and -1,79 m (RK 59). 1902 exact discharge at low water is unknown whereas one of 1962 is about 260 m^3/s. So, the differences between them may be attributable to a possible effect of the river bed incision phenomenon but also to a possible sensible discharge variation.

The river bed incision and the WL changes are also associated with an active channel narrowing of 44.8 % with an average width (main + side channels) reducing from 360 m to 199 m, with 13.7% due to side channel disappearance between 1860 and 1974 (Table 3).

Also, at the end of Phase 1, the DF patterns are essentially aquatic, lateral and complex. They are associated with low but variable terrestrialization rates of 28.3 ± 29.6% (Figure 8.b). Besides, the average relative elevation (RE) of the DFs to the WL is interesting to approach the channel-DF relationship: at the end of Phase 1, the 1962 RE of the DFs according to their pre-diversion terrestrialization percentages (GLM model) is associated with a $D^2 = 0.55$. In this relation, the more physically disconnected the DFs are from the WL, the more terrestrialized they are.

4.3.2. Phase 2: channelized and bypassed situation (1970s-2000s)

Between RK 52 and 63 of the study sub-sector, the river bed incision did not amplify (-0.13 m on average) during this phase 2 and so the longitudinal profile stabilized. On the other hand, a raising is observed upstream of the dam (max. at RK 50.5 with + 4 m) and a strong incision downstream of the sector when the Rhône is total again (average incision between RK 64 and 68 of -3.2 m and max of -5.1 m).

1962 WL with a mean annual flow and 2010 WL with a residual discharge are used to compare the situations in the average conditions before/after the installation of the diversion dam. The 1962 WL with a mean annual flow – just like 1962 WL with low water but higher on average of +1.62 m – evolves in a regular upstream-downstream elevation gradient. Flow diversion does not only cause a lowering of the WL due to the discharge reduction but also some WL slope changes. After a sudden fall at the level of the dam identified as Inflection Point 1 (IP1), the slope of the 2010 WL flattens (2010 WL $Slope_{RK51\text{-}59}$: 0.0165%) until meeting the Peyraud weir (IP 2 on Figure 8.a) where it falls and then flatten again. By comparing the 1962 and 2010 WL, if the two first IP are induced by the presence of the dam and the weir, the IP3 is marked by the fact that the slope is not recovering and the WL stays flat.

These WL changes are associated with an active channel narrowing of 10.4 %, the average width reducing from 199 m to 161 m (between 1974 and 2009). Currently, active channel only represents 45% of its 1860 area (Table 3).

Thus, the change in slope induces a change in the amplitude of the disconnection due to dewatering and the weir effect, by positively (between IP1 and IP3 except at the Peyraud weir location between RK 59 and RK 60.5) or negatively (before IP1, after IP3) incrementing the alluvial margins relative elevation according to the upstream-downstream gradient of the reach (Figure 8.b). The average delta between 1962 and 2010 WL resulted in an average dike field emersion of +2.22 m, with a maximum of +3.34 m at RK 52.4 just after the dam and a minimum of +0.98 at RK 62.9 not far before the IP3. Diversion-caused dewatering resulted by severely disconnecting the closed fields which are located relatively higher and more outside the channel (closed fields: RE_{WL2010} = 2.34 ± 1.03 m, Distance = 13 ± 11 m to the 2000s active

channel). In contrast, the opened fields are settled in the channel (open fields: RE_{WL2010} = 1.23 ± 0.84 m, D = 8.7 ± 15 m to the 2000s active channel but with an asymmetric distribution seeing as median distance = 0 m) and proportionally emerged to the channel narrowing according to location. Indeed, the rate of terrestrialization increase drastically directly after the flow diversion but remain very variable with regard to open fields (*cf.* TA% in open fields with a large distribution after diversion; observable on Figure 4).

The 2010 RE according to the post-derivation percentage of the dike fields (GLM model) is associated with a D^2 = 0.61. Thus, the more physically disconnected the DFs are from the WL, the more terrestrialized they are.

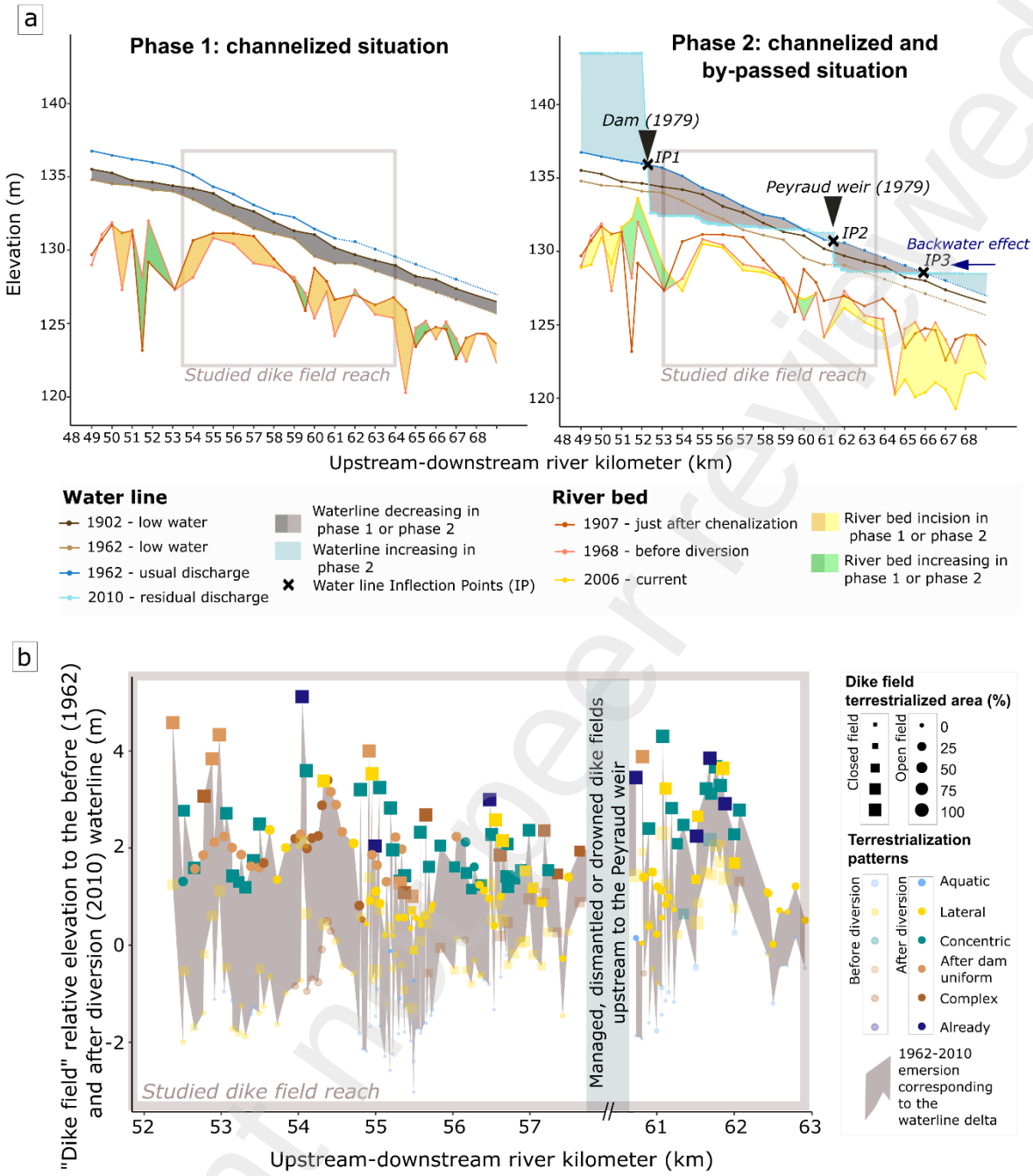

Figure 8: a. Upstream-downstream overview of the evolution of the water line and river bed elevation during phase 1 and phase 2 at PDR. State modalities for the water line survey are: during setting up the dike fields at low water (1902), before the establishment of the bypass at low and usual discharge (1962) and for the minimal flow (20m³/s in 2010) State modalities for the river bed survey are: just after setting up the dike fields (1907), before the diversion (1968) and about 28 years after diversion (2006) for the river bed survey (based on Parrot *et al.,* 2015); b. Before-after diversion dike field terrestrialization rates and patterns with regard to the water line change and the occurred emersion (comparison of the 1962 water line at the normal discharge and the 2010 water line at residual discharge); Note that for Figure 8.a. and 8.b., the WL 1962 (low and usual discharge) is only available between RK 48 and 60 and is extrapolated beyond.

Table 3: Active channel evolution at PDR from 1860 to 2009 (GIS survey)

		Date		
Parameters	**Objects on the PDR reach (11,12 km)**	**1860**	**1974**	**2009**
Area (ha)	Active channel (with side channels)	400,4	221,2	179,6
	Active channel (without side channel)	311,4	214,6	179,6
Width (m)	Active channel (with side channels)	360	199	161
	Active channel (without side channel)	280	193	161

4.4. Part of the diversion-caused "dewatering" in the terrestrialization

By inferring discharge-corresponding active channel surfaces from the "critical discharge leading to the pixel submersion" model (Figure 9.a), the active channel narrowing due to the drastic flow reduction was estimated. The difference between the occupied surfaces with the total average water discharge (1030 m^3/s) and the occupied surfaces at residual flow (20 m^3/s) (Figure 9.b), provide an estimate of the dewatered areas which were compared to the surfaces actually terrestrialized at this period from chronoplanimetric data (Figure 9.c).

In the studied area (8.5 km from RK 52), planimetric outcomes shows that terrestrialized areas directly after the flow diversion (1974-1982 sequence) correspond to 39.5 ha out of a total DF area of 82 ha (*i.e.,* 47% of the total area including terrestrial and aquatic areas). It represents 75% of the total terrestrialized area (1900s-2009) and 80% of the terrestrialized areas during phase 2 (1979-2009). It should be noted that this upstream sub-sector is characterized by a weaker terrestrialization in phase 1 and a much stronger one in phase 2 (*cf.* part 4.1.) than the rest of the reach because of its position along the longitudinal gradient that is more impacted by the flow diversion induced dewatering (Figure 8.a). In exactly the same sector and sample of DFs, the narrowing areas obtained thanks to the "critical discharge" model corresponds to 38.5 ha. The extent intersection of active channel retraction model and the 1974-1982 terrestrialized area amounts to 68% of common surfaces (*cf.* Figure 9.c; green area squared with yellow). This 32% difference may be due to errors in the model or to the fact that it is based on the DEM Lidar of 2010. Thus, the volumes occupied by the sediments deposited during the post-derivation period are not subtracted. This may affect the deployment of water volumes and incorporates an error since they are modeled to deploy on the current topography of the margins instead of the pre-diversion one because of a lack of historical DEM LIDAR. Also, in the phenomenon of terrestrialization, sedimentary deposition processes also

participate in the creation of new terrestrial areas, which could involve additional spaces that are included on the chronoplanimetry of the 1974-1982 sequence and not in the active channel narrowing model. Also, 3.2 ha have been modelized as terrestrialized when in reality they are still aquatic. These spaces notably correspond to the aquatic zones of the concentric patterns (*cf.* Figure 9.c, blue area).

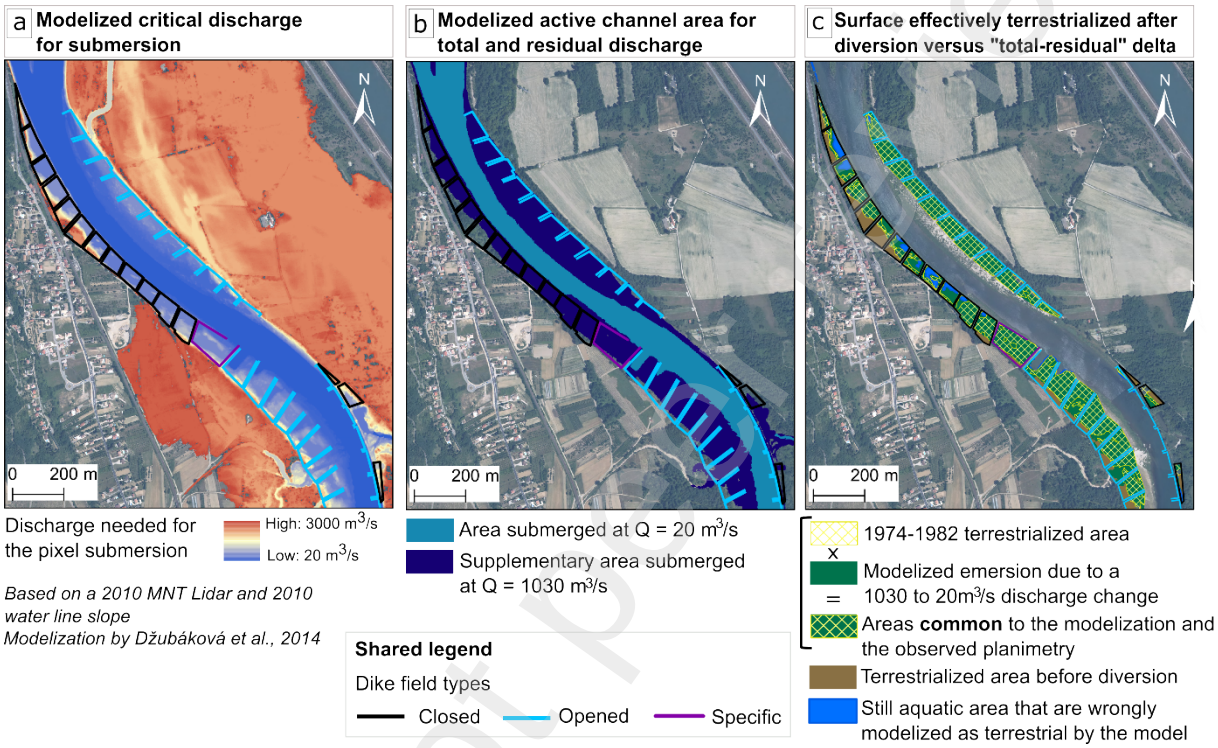

Figure 9: a. Modelized critical discharge for submersion of the alluvial margins and floodplain at PDR; b. Modelized active channel area corresponding to a total average discharge (1030 m3/s) and a residual discharge (20 m3/s) allowing; c. cross-checking of historical planimetry data and of the overflow-driven lateral submersion modelling (based on Džubáková *et al.,* 2014).

4.5. Current hydrological disconnexion versus local hydrological connectivity hot-spot associate to concentric patterns

The average submersion frequency of DFs (Figure 10.a) according to their terrestrialization percentages in 2009 (GLM model) is associated with a $D^2 = 0.68$. As predictable, the less the dike fields are hydrologically connected, the more they are terrestrialized. Nevertheless, the outputs showed that the concentric patterns did not fit the model (*cf.* Figure 10.a). In this model, the percentage of terrestrialization associated with this submersion frequency range overestimates the percentage actually observed for concentric patterns. When we remove the

concentric patterns of the dataset, the model reaches a D^2 of 0.78 (Dev =41.4, p-value = 1.237e-10).

Moreover, Minimum dike RE above the channel support this observation by displaying some enough low values with a strong variability (longitudinal dike minimum RE: 1.2 ± 0.7 m) for concentric patterns (Seignemartin, 2020).

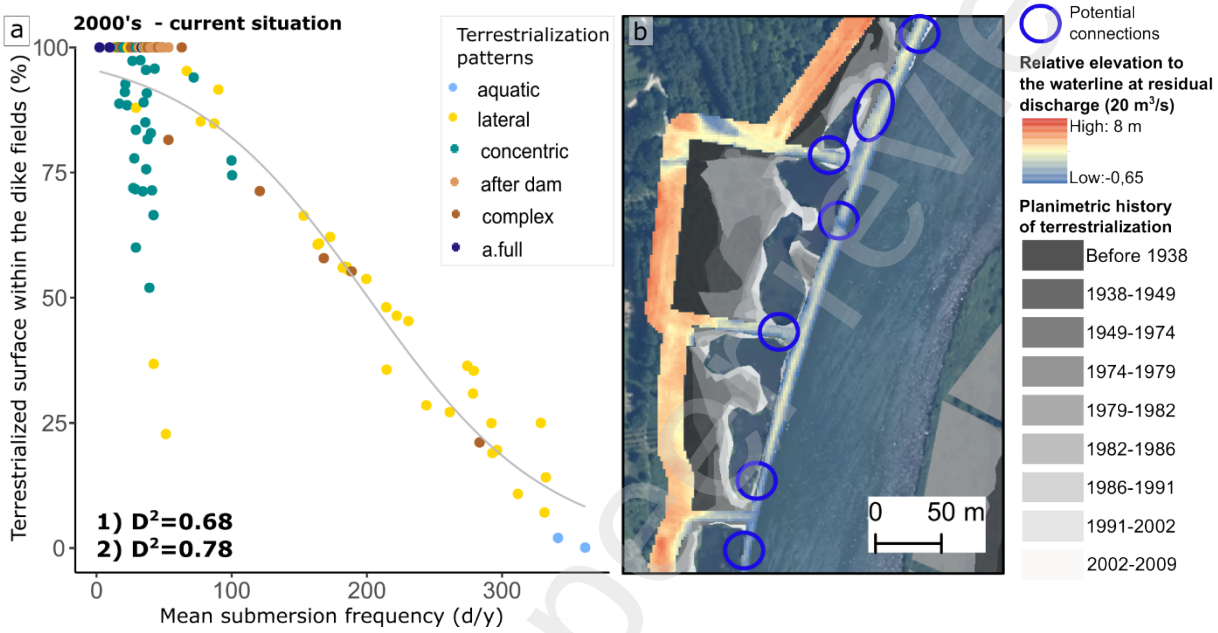

Figure 10: a. Current terrestrialized area according to mean overflow-driven lateral submersion frequency, associated GLM and highlighted exceptions of the concentric pattern type where D^2 (1) is calculated for the entire dataset, D^2 (2) excludes concentric patterns; b. Low spots, breaches in the dikes corresponding to potential hydrological connection points (based on 2010 Lidar DEM) at the level of closed fields with concentric patterns.

5. Discussion

5.1. About planform changes on the Rhône River and other highly engineered rivers

The assessment of geomorphological evolution based on GIS is often carried out at a larger scale as a part of an overall planform study (Arnaud *et al.,* 2015; Arnaud *et al.,* 2019; Piegay *et al.,* 2019; Tena *et al.,* 2020). By developing a specific georeferencing method consisting in using standardized georeferencing zones associated with recurrent “dike focused” ground control points, the bias due to deformations is reduced and the precision at the dike field scale is increased (low RMSE). The spatial and temporal accuracy of the obtained chronoplanimetry

then allows to distinguish several phases of the terrestrialisation phenomenon and patterns within the dike fields.

The quantitative data (terrestrialized area and active channel narrowing) show that there is a first “post-channelization” (1900s-1970s) phase with a system that adjusts to these first deep changes. It corresponds to a terrestrialization of their cumulated areas reaching 47% in closed fields and 16% in opened fields. Such a trajectory was already observed at the PDR reach scale: the main and side channels present a surface decrease reaching 40% after the channelization phase (1810-1938 area loss). After the diversion phase, it is a 20% additional loss of surface for the main and side channels, *i.e.,* a total loss of 60% during these two last centuries (Tena *et al.,* 2020). In the dike fields, the second phase (after the dam diversion) is associated with a terrestrialization of 32 % in closed fields and 51% in opened fields of their areas. In total, after the two phasis of engineering developments, these are 79% closed field and 67% of opened field areas that have been terrestrialized. Thus, compared to the previous overall “floodplain” assessment, DF terrestrialization percentages are quite similar or higher.

These results are in accordance to those find in the literature. For example, an average channel width narrowing of 60% is observed between 1826 and 1991 on the Danube River which has also been channelized (study reach extent: 10.25 km; Hohensinner *et al.,* 2004). On the Piave River (Italy), that is much engineered with streambank protection structures, hydroelectric dams (study reach extent: 110 km; Surian, 1999) a 58 to 70% active channel narrowing was reported. On the Dordogne river in France (study reach extent: 162 km), the 12,2% active channel retraction from 1948 to 2012 was interpreted as combined effects of streambank protection structures, regulation and sediment extractions (Boutault, 2020). At the scale of groyne fields on the Danube River, Savic *et al.* (2013) observed that 40 to 80% of the surfaces were currently filled with fluvial sediment materials. Thus, compared to other rivers and alluvial compartments, the Rhône River DFs – which are a specific and very constrained part of the engineered margins – have recorded a particularly drastic phenomenon of terrestrialization. Nevertheless, surface losses of floodplain aquatic areas are even more

766 drastic in the former side channels of the Rhône River by reaching 90% during the few last
767 decades (Depret et al, 2017).

768 ### 5.2. Hydromorphologic processes underlying the phase 1: channelized
769 ### situation (1900s-1970s)

770 Riverbed incision is an expected and commonly observed impact on channelized rivers (*e.g.,*
771 Wyżga, 2001; Brierley and Fryirs, 2005; Kroes and Hupp, 2010). Indeed, the purpose of the
772 DFs was to cause the channel to retract and concentrate the shear stresses in the center so
773 that it would deepen, thereby increasing the draft and promoting navigation conditions
774 (Girardon, 1883; Fruget, 1992). In this way, during the first phase, the channelization could
775 have definitely influenced the emergence of the surfaces adjacent to the active channel. In the
776 case of PDR, we can observe a channel narrowing and a simplification of channel geometry.
777 Also, the difference between 1902 and 1962 WL at low water shows a slight lowering of 1,07
778 m that can be a little more or less pronounced according to the potential difference of discharge
779 between low water of 1962 – 260 m^3/s – and 1902, unknown). Although all these
780 hydromorphologic changes could indicate a riverbed incision (Simon and Rinaldi, 2006;
781 Zawiejska and Wyżga, 2010; Arnaud *et al.,* 2015; Parrot, 2015), PDR remains relatively
782 preserved (average elevation delta between 1897 and 1969 of -0,92 m) in comparison to other
783 sectors of the Rhône River (*e.g.,* Pierre-Bénite reach: -4,05 m), even if it can reach high value
784 locally (max. of the reach: -3.41 m at RK 59). The bypassed reaches experienced an increase
785 in in-channel shear stresses with the channelization, so they experienced a phenomenon of
786 bedload transport leading to reduction and riverbed incision. At the PDR, shear stresses in the
787 channel likely increased with channelization but - in a cascade effect - the available sediment
788 load provided by the upstream channelized portion would offset the potential imbalance
789 between shear stresses and available sediment. This explains the moderate incision. On the
790 other hand, the Pierre-Bénite reach is located in the upstream part of the channelization work
791 and therefore does not benefit from the cascade effect and the associated upstream sediment
792 supply.

Also, if shear stresses have increased within the channel, DFs delimit areas where they are reduced. By relying on the types of vegetation in their biogeomorphic function, it is possible to attest of hydro-sedimentary tendencies (Bendix and Hupp, 2000; Corenblit *et al.,* 2009). According to the diachronic photograph series (Figure 2) and previous studies (Seignemartin, 2020), sediment deposits located at the back of closed fields are terrestrialized and vegetated since the first photographs (Figure 2: 1938, left bank). They seemed rather stable – slightly increasing – and so, subject to limited scouring processes that remains weak enough to allow development of trees (Figure 2: 1938, 1949 and 1974 series; Figure 3: associated quantitative data). Open fields are for many aquatic but for those who have begun to terrestrialize (*e.g.,* on Figure 2, right bank), the situation is quite similar to that observed on more flooded habitat such as gravel bars (Gilvear and Willby, 2006; Francis *et al.,* 2006). They present open areas that are under fluctuating water levels and stronger erosive processes where pioneer vegetation can be sometimes observed (mainly herbaceous and shrubby layers*;* Seignemartin, 2020). The bareness of these sedimentary deposits or even the presence of pioneer vegetation indicates greater instability and hydrological disturbance than where woody vegetation is able to develop (Malanson, 1993; Corenblit *et al.,* 2009). In this situation, closed and opened fields during the first half of the 20th century seem hydrologically connected to the channel and subject to deposition and erosive processes according to magnitude of flood disturbance. The morphological context (concavity, convexity, rectilinear zone), the density and specificities of the DF – *e.g.,* relative elevation, geometry, type (open field versus closed fields), or the characteristics of the closed field longitudinal dike such as its height, can explain local variations in terrestrialization patterns, in particular by playing on shear stress conditions and hydraulic recirculation patterns (Copeland, 1983; Sukhodolov *et al.*, 2002). The GPR surveys also show that sediment internal structures are much more pronounced in the open fields. Subjects to more shear stresses, they present sediment patterns that are more contrasted (thicker reflectors on the radargrams; Figure 6 - GPR T3) associated with coarser grain size (e.g., case of the plunge pool downstream of groynes that are typical of energy dissipation gradients; Figure 6 - GPR T3). On the contrary, closed fields showed a greater propensity for

fine sediment accretion along its distal side, probably due to the longitudinal dike and groynes limiting shear stress.

In conclusion, geomorphological and biomorphic trajectories highlight the control factors of the terrestrialization during phase 1. At PDR, although it is possible that the incision had a slight impact – locally more or less pronounced – the terrestrialization seems to be driven by sediment accretion processes due to the limitation of shear stresses in the DFs.

5.3. Hydromorphologic processes underlying the phase 2: channelized and bypassed situation (1970s-2000s)

During phase 2, the incision is not amplified on the studied section (average elevation delta between 1969 and 2009 of -0,13 m). Thus, the water level evolutions are almost entirely attributable to the establishment of the bypassed reach in 1977. In this case, the flow reduction in the bypassed reach has probably reduced in-channel shear stress; and mitigate incision tendencies. A similar trend was observed on an old Rhine bypassed section by Arnaud *et al.* (2015). On the other hand, we observe at PDR a phenomenon of pre-dam river bed aggradation (depositional pattern) and post-dam incision (erosional pattern) (Figure 8.a – Phase 2). It is a common morphological adjustment on engineered rivers of the northern hemisphere: the dam reservoir leads to favorable conditions for sedimentary accumulation, while downstream, the constraints caused by the flow, which has become total again, create conditions favorable to incision (Kondolf, 1997; Ibisate *et al.,* 2013).

In the bypassed reach, the flow reduction had the direct effect of causing a dewatering leading to the emersion of the channel edge areas. It also leads to a lowering and a change in slope of the WLs, implying that margin emersion is expressed differentially according to the upstream-downstream gradient depending on the angle of the change in slope (Figure 9.a and 9.b). To this upstream-downstream pattern is added the effect of the Peyraud weir, creating an inflection point (IP 2 on Figure 9.b) which instigates new gradients at 2/3 of the reach. Its installation in 1979 involved the dismantling and/or submersion of certain structures (*cf.* Figure 8.a., RK 59 to 60.5 at the Peyraud weir) which explains the absence of DFs studied at this

level. Finally, a backwater effect maintains and prolongs the flattening downstream of the water line. In this case, it is the downstream connection of the bypassed reach with the main channel which is impacted by the next downstream reservoir on the river. This phenomenon is typical of bypassed configurations (Lamouroux *et al.,* 1999).

Within the reach, the longitudinal gradient of the water line is therefore marked by the dam, the weir and the backflow effects. Therefore, the channel-alluvial margins connection relationship evolves (in time and space) differently along this gradient. This differential hydrological connection can be an additional explanatory factor for local variability within more global trends of terrestrialization. It is added to the complexity associated to morphological context, density and geometrical characteristics of the DFs that can influence the hydrological connection and shear stress parameters of engineered margins.

After the flow diversion (1979), alluvial margins are then under the two-development impact by being corseted and less hydrologically connected because of the regulation. Therefore, the already accreted and/or dewatered surfaces are more inclined to encroached by terrestrial vegetation that can increase roughness and store fine sediments which will not be remobilized as the erosive processes are reduced under regulated flood conditions. The GPR radargrams testify that there are recent deposits (*e.g.,* upper layers on the radargrams associated with recent chronoplanimetric sequences, Figure 6) with a finer texture than previous deposits. On the Rhône River, it is in line with the literature about overbank fine sediment storage in areas enduring a loss of hydrological connectivity (Citterio and Piégay, 2009; Arnaud *et al.,* 2015; Tena *et al.*, 2020; Vauclin *et al.,* 2020). Also, the roughness due to vegetation encroachment is favorable to increase fine sediment accretion (Arnaud *et al.,* 2015). Indeed, vegetated surfaces (herbaceous, shrubs and trees) evolve from 32.4% in 1974 to 55.2% in 1986 and then stabilized around 61 % on the 1991 and 2009 series (Seignemartin, 2020). This adjustment dynamic during phase 2 – whether in terms of channel narrowing, terrestrialization or vegetation – is typical of post-dam adjustment trajectories. The initial response is intense

and followed by a of asymptotic relaxation (Graf, 1977; Surian and Rinaldi, 2003; Petts and Gurnell, 2005; Arnaud *et al.,* 2015).

Also, according to Janssen *et al.* (2020), the current tree density in closed fields testifies to rare disturbances spaced out over time: the wooded areas have increased over time and so has the specific diversity. There is in particular the appearance of hardwood species, typical of secondary successions (*e.g., Fraxinus angustifolia, Ulmus minor, Acer campestre)* which develop in within a riparian forest initially composed of softwood species (*e.g., Populus alba, Populus nigra, Salix alba*). Gradual disappearance of the recruitment niches of these tree species testify to a hydrologically disconnected alluvial environment. In open fields, the vegetation encroachment of shrubby layers is also more important on post-diversion terrestrialized surfaces (Seignemartin, 2020). These observed vegetation patterns are evidence that alluvial margins are characterized by overall hydrologic disconnection and that only vegetation very close to the channel is representative of riparian habitat (Malanson, 1993; Corenblit et al., 2009; Corenblit et al., 2014). (Malanson, 1993; Corenblit *et al.,* 2009; Corenblit *et al.,* 2014).

To the impacts of developments on the studied section are added the pressures and their impacts on the scale of the Rhône watershed (*e.g.,* gravel mining in the active channel until the 1990s). Also, Vázquez-Tarrío *et al.* (2018) showed in particular that a multi-dam series can have a cumulative impact on sediment transfers and geomorphic interaction between successive reaches; which is our case here because the PDR reach corresponds to the second diversion dam of a series of eleven between Lyon and the Mediterranean Sea.

5.4. From deposition patterns to terrestrialization ones: correspondences, specificity and contribution of the chronoplanimetric approach

A classic reference in the field is the classification of sediment deposition patterns established by Sukhodolov *et al.* (2002) from flume experiments and observations on the Elbe River. Based on the proportion of filling and the deposition forms, their inter-groyne typology presents seven

patterns that are also observable in our classification (*cf.* Figure 11 and Table 4). Our aquatic type can refer to the "weak deposition" of Sukhodolov. Lateral patterns gathered many forms found in Sukhodolov typology: "upstream" and "downstream triangle shaped deposition", "upstream" and "downstream wave shaped deposition", "uniform partial" and "complete deposition". Our typology does not segregate them because the approach here tends to break away from local hydraulic controls and enlighten the impact of the main fluvial modifications. Indeed, the objectives of Sukhodolov *et al.* (2002) were to make the link between flow recirculation and sedimentary deposition at one date and a local scale whereas we seek to highlight at the cumulative developments that lead to terrestrialization over a century at a reach scale.

In addition to these corresponding patterns, there are additional ones that are related to the Rhône River engineering developments and geomorphological specificities. Indeed, the case of closed fields which presence of the longitudinal submersible dike might complexify the hydrological connection terms and play on scour patterns by involving other parameters (dike height, possible dike breach, etc.). One of the main pattern particularities of closed fields is the recurrence of concentric type that is observed with two current states: semi-aquatic with pool within the concentric shapes or fully terrestrialized. In the semi-aquatic case, the current hydrological connectivity is underestimated by the average submersion frequency of DFs (Figure 9.a). Indeed, that kind of patterns seems to be conditioned by breaches or lower spots in the dike that induce water inlets (Figure 9.b) which instigate circulating flows, scouring patterns with enough shear stress to shape concentric forms and associated water ponds for still aquatic ones (Figure 9.b). For fully terrestrialized one, chronoplanimetries show that they become terrestrial shortly after flow diversion. They are associated with former concentric water pool that fill up with fine sediments (Figure 6 - GPR T2). Uniform type is another additional pattern that retranscribes the direct effect of the flow diversion and its associated dewatering (Figure 8.c).

Also, local variability (presence of former side channels, old islands, etc.) is associated with "complex shapes" of which surface is more or less terrestrialized and which patterns evolve

according to the initial form implied by the geomorphological specificities (*e.g.,* accretion around an old island, within former side channels).

This GIS approach provides terrestrialization patterns that are diachronic on a very large sample of DFs. They endow a whole spatio-temporal dimension which provides information on local particularities but also on the overall transformations of the alluvial margins. After identifying major changes, it would be possible to focus on intra-class variation of patterns, notably by studying the DF geometric parameters and hydraulic indicators. GIS produced datasets could also be computed with existing hydraulic model outcomes (*e.g.,* in Copeland, 1983; Sukhodolov *et al.,* 2002; McCoy, 2006).

Moreover, the relevance of a planimetric approach to characterize sedimentary deposits is validated by the comparison of planimetric patterns with topography (Figure 7.a). It confirms the methodology but also offers an interesting tool for the chronological characterization of sedimentary deposits, taking the characterization towards 4D.

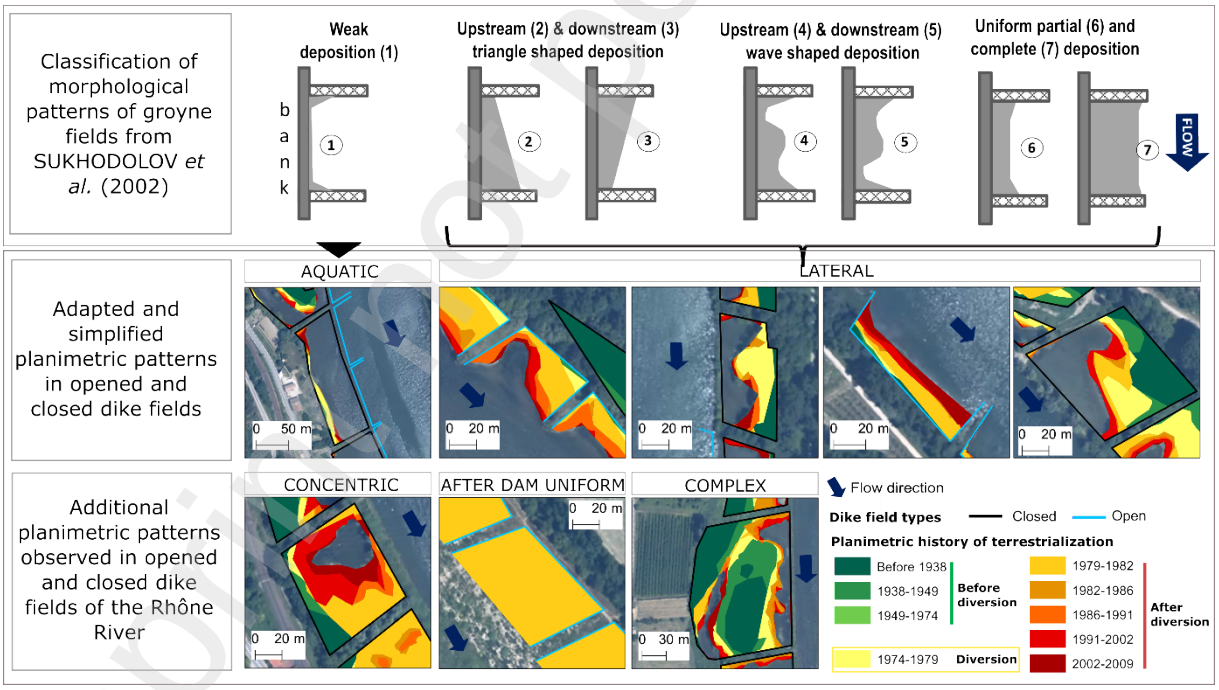

Figure 11: Comparison of the terrestrialization patterns within the dike fields at PDR and the inter-groynes deposit patterns of Sukhodolov *et al.* (2002)

947 Table 4 : Classification of terrestrialization patterns and Sukhodolov correspondences

Type	Description	Correspondence to the Sukhodolov classification
Aquatic	The surface of the dike structure is mainly aquatic (aquatic surface > 85% of the dike structure extent).	Weak deposition
Lateral	The surface of the dike structure is partially terrestrialized; laterally to the bank.	Upstream & downstream triangle shaped deposition Upstream & downstream wave shaped deposition Uniform partial and complete deposition
Concentric	The surface of the dike structure is highly terrestrialized. Areas with progressive concentric closures may remain aquatic.	No correspondence Additional pattern observed in closed field
After dam uniform	The surface of the dike structure corresponds to a uniform terrestrialized band caused by the lowering of the water line (after diversion).	No correspondence Additional pattern due to diversion
Complex	The surface of the dike structure is more or less terrestrialized. Stationary variability (presence of former side channels, old islands, original dike configurations, etc.) causes complex forms.	No correspondence Additional pattern due local complexity

948

949 ## 5.5. Implications for adapted river restoration measures

950 DF terrestrialization constitutes a logical channel response to the Rhône River hydrological
951 disconnection. In a distal logic, it first affected the side channels (Citterio and Piégay, 2009;
952 Riquier *et al.,* 2017), then the distal part of DFs and ended up affecting the DF proximal areas
953 with different situations according to local shear stress changes and effects of new
954 infrastructures on longitudinal water level. If the DF could have been thought of as aquatic
955 functional relays to the side channel (Thorel *et al.* 2018; Franquet, 1999), they lose their
956 potential as fluvial annexes (refuge habitats) once they have become terrestrial. In contrast,
957 their primary function is still at work since they continue to constrain the alluvial margins,
958 impacting alluvial functionality and questioning their future within the framework of ecological
959 restoration programs (Räpple, 2018; Thorel *et al.,* 2018).

960 At the level of the connected dike fields, the zones of privileged hydrological connection allow
961 the maintenance of aquatic and concentric patterns making these dike fields which come
962 closest to the concept of “novel ecosystem” (Morse *et al.,* 2014). These features present hydro-
963 sedimentary dynamics that seem to be the most in a new equilibrium under current functional
964 conditions since these allow them to preserve a semi-aquatic character; all consideration kept
965 of an incision context and forecasting of water discharge decrease. At the level of concentric
966 patterns that are fully terrestrialized, there are residual pits inherited from before-dam erosive
967 dynamics, then filled with fine sediments (Figure 6 - GPR A). Thereby, these pools are

representative of a high connectivity which allows water inputs with enough smooth erosive processes to maintain fine sediment deposits but no longer sufficient to maintain aquatic pools. They draw attention to the fact that there is a hydrological connectivity threshold that could be assessed. Currently restoration programs are on a bimodal restoration strategy between DF conservation or dismantling. It would be interesting to elaborate a further adaptative strategy aiming to recreate hydrological connectivity gradients favorable to a mosaic of semi-aquatic habitats. It would imply a dike field reconnection model – inspired by the effective side channel reconnection strategies (Riquier *et al.,* 2017) – via lowering or removing certain dikes in order to maintain ecotones that have a high potential for biological diversity and ecological functioning (Risser, 1990; Naiman and Décamps, 1997; Ward *et al.* 1999). A work of modulation of instream flow in the bypassed could also make possible to recreate the necessary hydrological connections.

These operational prospects are to be considered taking into account overall trajectories, in particular the potential effect of climate change on environmental and socio-economic systems. It would notably impact magnitude and timing of streamflow (Beniston, 2012; Beniston and Stoffel, 2014; Clarvis *et al.,* 2014; Rahman *et al.,* 2015). Flow regulation is under control in the bypassed sections and might be impacted by management changes, notably with a potential increase of extreme events (Beniston and Stoffel, 2014). Already impacted by by-pass dam and pumping, water table sinking and retraction has caused less hydromorphic conditions that have affected riparian vegetation development and community composition (Dufour, 2007). The non-bypassed parts but also the intake channels could be subject to streamflow reduction. In this case, a potential retraction of the water table could lead to gradual dewatering and an alteration of groundwater-alluvial areas interactions; exacerbating even more the floodplain hydrological disconnection at a larger scale.

This approach also provides sediment diagnosis useful in the framework of restoration programs. For example, at PDR in a sub-sample of 147 DFs defined for restoration purposes, volumes of 675,000 m^3 of fine sediment overlaying 723,500 m^3 of coarse sediment are

estimated, spread over a cumulated area of 77.1 ha. Allowing a 4D characterization of the alluvial margins, this cross-validation (geohistory-geophysics) could guide the sanitary assessment by prioritizing the sampling of terrestrialized areas where the chronology of contaminant flow peaks is concomitant with (Seignemartin *et al.,* 2022).

6. Conclusion

Updating the study of infrastructure “sediment deposition", intra-dike field terrestrialization patterns by GIS shed light on the prevalence of engineering developments in their evolutionary trajectories by controlling hydrosedimentary and vegetation processes within the dike fields and in the main river channel.

The Rhône River chenalization transformed the multi-thread channel into a single channel, marked by a shear stress concentration in the main stem with more or less incision (*e.g.,* low at PDR compared to other bypassed Rhône River reaches, cf. Parrot, 2015) and the set-up of new semi-aquatic engineered alluvial margins. The DFs have then experienced a first stage of partial terrestrialization which may be due to a sedimentation along the distal edge of DFs due to shear stress reduction. The second phase initiated by the flow diversion participates directly to the margin terrestrialization: cross-checking of models underlines that diversion-induced dewatering has provoked the emersion of almost the half of the DF extent on the upper part of the studied reach (75% of the total terrestrialized area). It also modifies drastically the hydrological connectivity of the floodplain. So, the margins are even less hydrologically connected and therefore more inclined to vegetation encroachment, roughness increase and fine sediment deposits which will not be remobilized (erosive processes reduced under regulated flood flows). This is even more exacerbated by peak flow magnitude and recurrence decrease following derivation, reducing shear stress in the DFs.

The DF terrestrialization is ending up telling the story of a drastic disconnection of the Rhône River from its riparian ecosystem, become a rarely “flooded” plain. Indeed, it constitutes an expected extension to the phenomenon of hydrological disconnection of the Rhône River which, in a distal logic, first affected the side channel and progressively the DFs, then that get

carried away with the second development phase and ended up by affecting the proximal channel margins. Therefore, it led to an area reduction of side channels, a loss of semi-aquatic features and therefore their ecotone and refuge habitat functionalities. Concerning the rehabilitation masterplans, a dike field reconnection in line with hydrological reality (a strategical dike removal or lowering) could support the river in recreating gradients of hydrological connectivity that it is no longer capable of creating or maintaining on its own. In this context of profound modifications of rivers to the point that we qualified them of "anthropocene rivers", it is essential to assess the evolutionary trajectories of these anthropo-ecosystems in order to target ecosystemic dysfunctions and lost functionalities with a view to proposing some functional(ity) rehabilitation measures adapted the hydro-sedimentary reality of river systems.

7. Acknowledgment

This study was conducted as part of the Rhône Sediment Observatory (OSR) program, a multi-partner research program funded through Plan Rhône of the European Regional Development Fund (ERDF), Agence de l'Eau Rhône Méditerranée Corse, CNR, EDF and three regional councils (Region Auvergne-Rhône-Alpes, PACA and Occitanie). The work was performed within the framework of the EUR H2O'Lyon (ANR-17-EURE-0018) of Université de Lyon (UdL) through the “Investissements d'Avenir” program operated by the French National Research Agency (ANR) and through Labex DRIIHM, French programme “Investissements d'Avenir” (ANR-11-LABX-0010) managed by the ANR of the Observatoire Hommes-Milieux Vallée du Rhône (OHM VR). We would like to thank the EVS 5600 Laboratory staff and partners, Katarína Džubáková, Mélanie Bertrand, Alvaro Tena, Bianca Räpple, Robin Gruel, Pierre-Hugo Lecomte.

8. References

Amoros, C., Bornette, G., 2002. Connectivity and biocomplexity in waterbodies of riverine floodplains: Connectivity and biocomplexity in riverine floodplains. Freshwater Biology 47, 761–776. https://doi.org/10.1046/j.1365-2427.2002.00905.x

Arnaud, F., Piégay, H., Schmitt, L., Rollet, A.J., Ferrier, V., Béal, D., 2015. Historical geomorphic analysis (1932–2011) of a by-passed river reach in process-based restoration perspectives: The Old Rhine downstream of the Kembs diversion dam (France, Germany). Geomorphology 236, 163–177. https://doi.org/10.1016/j.geomorph.2015.02.009

Arnaud, F., Schmitt, L., Johnstone, K., Rollet, A.-J., Piégay, H., 2019. Engineering impacts on the Upper Rhine channel and floodplain over two centuries. Geomorphology 330, 13–27. https://doi.org/10.1016/j.geomorph.2019.01.004

Arnaud, F., Sehen Chanu, L., Grillot, J., Riquier, J., Piégay, H., Roux-Michollet, D., Carrel, G., Olivier, J.-M., 2021. Historical cartographic and topo-bathymetric database on the French Rhône River (17th–20th century). Earth Syst. Sci. Data 13, 1939–1955. https://doi.org/10.5194/essd-13-1939-2021

Belletti, B., Garcia de Leaniz, C., Jones, J., Bizzi, S., Börger, L., Segura, G., Castelletti, A., van de Bund, W., Aarestrup, K., Barry, J., Belka, K., Berkhuysen, A., Birnie-Gauvin, K., Bussettini, M., Carolli, M., Consuegra, S., Dopico, E., Feierfeil, T., Fernández, S., Fernandez Garrido, P., Garcia-Vazquez, E., Garrido, S., Giannico, G., Gough, P., Jepsen, N., Jones, P.E., Kemp, P., Kerr, J., King, J., Łapińska, M., Lázaro, G., Lucas, M.C., Marcello, L., Martin, P., McGinnity, P., O'Hanley, J., Olivo del Amo, R., Parasiewicz, P., Pusch, M., Rincon, G., Rodriguez, C., Royte, J., Schneider, C.T., Tummers, J.S., Vallesi, S., Vowles, A., Verspoor, E., Wanningen, H., Wantzen, K.M., Wildman, L., Zalewski, M., 2020a. More than one million barriers fragment Europe's rivers. Nature 588, 436–441. https://doi.org/10.1038/s41586-020-3005-2

1073 Bendix, J., Hupp, C.R., 2000. Hydrological and geomorphological impacts on riparian plant
1074 communities. Hydrol. Process. 14, 2977–2990. https://doi.org/10.1002/1099-
1075 1085(200011/12)14:16/17<2977::AID-HYP130>3.0.CO;2-4

1076 Beniston, M., 2012. Impacts of climatic change on water and associated economic activities in
1077 the Swiss Alps. Journal of Hydrology 412–413, 291–296.
1078 https://doi.org/10.1016/j.jhydrol.2010.06.046

1079 Beniston, M., Stoffel, M., 2014. Assessing the impacts of climatic change on mountain water
1080 resources. Science of The Total Environment 493, 1129–1137.
1081 https://doi.org/10.1016/j.scitotenv.2013.11.122

1082 Beres Jr., M., Haeni, F.P., 1991. Application of ground-penetrating-radar methods in
1083 hydrogeologic studies. Ground Water 29, 375–386. https://doi.org/10.1111/j.1745-
1084 6584.1991.tb00528.x

1085 Beres, M., Huggenberger, P., Green, A.G., Horstmeyer, H., 1999. Using two- and three-
1086 dimensional georadar methods to characterize glaciofluvial architecture. Sedimentary Geology
1087 129, 1–24. https://doi.org/10.1016/S0037-0738(99)00053-6

1088 Boutault, F., 2020. Etude de l'impact cumule des facteurs d'anthropisation sur la Dordogne
1089 moyenne et préconisations en vue de la restauration écologique du cours d'eau. Unpublished.

1090 Bravard, J.-P., 2010. Discontinuities in braided patterns: The River Rhône from Geneva to the
1091 Camargue delta before river training. Geomorphology 117, 219–233.
1092 https://doi.org/10.1016/j.geomorph.2009.01.020

1093 Bravard, J.-P., Amoros, C., Pautou, G., 1986. Impact of Civil Engineering Works on the
1094 Successions of Communities in a Fluvial System: A Methodological and Predictive Approach
1095 Applied to a Section of the Upper Rhône River, France. Oikos 47, 92.
1096 https://doi.org/10.2307/3565924

1097 Brierley, G.J., Fryirs, K.A. (Eds.), 2004. Geomorphology and River Management. Blackwell
1098 Publishing, Malden, MA, USA. https://doi.org/10.1002/9780470751367.fmatter

1099 Brooker, M.P., 1985. The Ecological Effects of Channelization. The Geographical Journal 151,
1100 63. https://doi.org/10.2307/633280

1101 Brookes, A., 1985. traditional engineering methods, physical consequences and alternative
1102 practices. Progress in Physical Geography: Earth and Environment 9, 44–73.
1103 https://doi.org/10.1177/030913338500900103

1104 Bryant, R.G., Gilvear, D.J., 1999. Quantifying geomorphic and riparian land cover changes
1105 either side of a large flood event using airborne remote sensing: River Tay, Scotland.
1106 Geomorphology 29, 307–321. https://doi.org/10.1016/S0169-555X(99)00023-9

1107 Buczyńska, E., Szlauer-Łukaszewska, A., Czachorowski, S., Buczyński, P., 2018. Human
1108 impact on large rivers: the influence of groynes of the River Oder on larval assemblages of
1109 caddisflies (Trichoptera). Hydrobiologia 819, 177–195. https://doi.org/10.1007/s10750-018-
1110 3636-6

1111 Citterio, A., Piégay, H., 2009. Overbank sedimentation rates in former channel lakes:
1112 characterization and control factors. Sedimentology 56, 461–482.
1113 https://doi.org/10.1111/j.1365-3091.2008.00979.x

1114 Copeland, R.R., n.d. Bank Protection Techniques Using Spur Dikes 36.

1115 Corenblit, D., Steiger, J., González, E., Gurnell, A.M., Charrier, G., Darrozes, J., Dousseau, J.,
1116 Julien, F., Lambs, L., Larrue, S., Roussel, E., Vautier, F., Voldoire, O., 2014. The
1117 biogeomorphological life cycle of poplars during the fluvial biogeomorphological succession: a
1118 special focus on *Populus nigra* L. Earth Surf. Process. Landforms 39, 546–563.
1119 https://doi.org/10.1002/esp.3515

Corenblit, D., Steiger, J., Gurnell, A.M., Tabacchi, E., Roques, L., 2009. Control of sediment dynamics by vegetation as a key function driving biogeomorphic succession within fluvial corridors. Earth Surf. Process. Landforms 34, 1790–1810. https://doi.org/10.1002/esp.1876

Davis, J.L., Annan, A.P., 1989. Ground-penetrating radar for high-resolution mapping of soil and rock stratigraphy. Geophys Prospect 37, 531–551. https://doi.org/10.1111/j.1365-2478.1989.tb02221.x

Dépret, T., Riquier, J., Piégay, H., 2017. Evolution of abandoned channels: Insights on controlling factors in a multi-pressure river system. Geomorphology 294, 99–118. https://doi.org/10.1016/j.geomorph.2017.01.036

Dufour, S., 2007. Contrôles hydro-morphologiques et activités anthropiques dans les forêts alluviales du bassin rhodanien: Annales de géographie n° 654, 126–146. https://doi.org/10.3917/ag.654.0126

Dynesius, M., Nilsson, C., 1994. Fragmentation and Flow Regulation of River Systems in the Northern Third of the World. Science 266, 753–762. https://doi.org/10.1126/science.266.5186.753

Džubáková, K., Piégay, H., Riquier, J., Trizna, M., 2015. Multi-scale assessment of overflow-driven lateral connectivity in floodplain and backwater channels using LiDAR imagery. Hydrol. Process. 29, 2315–2330. https://doi.org/10.1002/hyp.10361

Elawady, E., Michiue, M., Hinokidani, O., 2001. Movable bed scour around submerged spur-dikes. Proceedings Of Hydraulic Engineering 45, 373–378. https://doi.org/10.2208/prohe.45.373

Francis, R.A., Gurnell, A.M., Petts, G.E., Edwards, P.J., 2006. Riparian Tree Establishment on Gravel Bars: Interactions between Plant Growth Strategy and the Physical Environment, in: Sambrook Smith, G.H., Best, J.L., Bristow, C.S., Petts, Geoff E. (Eds.), Braided Rivers.

Blackwell Publishing Ltd., Oxford, UK, pp. 361–380. https://doi.org/10.1002/9781444304374.ch18

Franquet, E., 1999. Chironomid assemblage of a Lower-Rhone dike field: Relationships between substratum and biodiversity. Hydrobiologia 397, 121–131. https://doi.org/10.1023/A:1003681817806

Fruget, J.F., 1992. Ecology of the lower Rhône after 200 years of human influence: A review. Regul. Rivers: Res. Mgmt. 7, 233–246. https://doi.org/10.1002/rrr.3450070303

Fryirs, K.A., Brierley, G.J., 2012. Geomorphic Analysis of River Systems: An Approach to Reading the Landscape. Wiley.

Gawthorpe, R.L., Collier, R.E.L., Alexander, J., Bridge, J.S., Leeder, M.R., 1993. Ground penetrating radar: application to sandbody geometry and heterogeneity studies. Geological Society, London, Special Publications 73, 421–432. https://doi.org/10.1144/GSL.SP.1993.073.01.24

Geerling, G.W., Ragas, A.M.J., Leuven, R.S.E.W., van den Berg, J.H., Breedveld, M., Liefhebber, D., Smits, A.J.M., 2006. Succession and Rejuvenation in Floodplains along the River Allier (France). Hydrobiologia 565, 71–86. https://doi.org/10.1007/s10750-005-1906-6

Gilvear, D., Bryant, R., 2003. Analysis of aerial photography and other remotely sensed data. Tools in fluvial geomorphology 5, 23.

Gilvear, D., Willby, N., 2006. Channel dynamics and geomorphic variability as controls on gravel bar vegetation; River Tummel, Scotland. River Res. Applic. 22, 457–474. https://doi.org/10.1002/rra.917

Graf, W.L., 1977. The rate law in fluvial geomorphology. American Journal of Science 277, 178–191. https://doi.org/10.2475/ajs.277.2.178

Gregory, K.J., 2006. The human role in changing river channels. Geomorphology 79, 172–191. https://doi.org/10.1016/j.geomorph.2006.06.018

1169 Gurnell, A.M., 1997. Channel change on the River Dee meanders, 1946–1992, from the
1170 analysis of air photographs. Regul. Rivers: Res. Mgmt. 13, 13–26.
1171 https://doi.org/10.1002/(SICI)1099-1646(199701)13:1<13::AID-RRR420>3.0.CO;2-W

1172 Hobbs, R.J., Arico, S., Aronson, J., Baron, J.S., Bridgewater, P., Cramer, V.A., Epstein, P.R.,
1173 Ewel, J.J., Klink, C.A., Lugo, A.E., Norton, D., Ojima, D., Richardson, D.M., Sanderson, E.W.,
1174 Valladares, F., Vilà, M., Zamora, R., Zobel, M., 2006. Novel ecosystems: theoretical and
1175 management aspects of the new ecological world order: Novel ecosystems. Global Ecology
1176 and Biogeography 15, 1–7. https://doi.org/10.1111/j.1466-822X.2006.00212.x

1177 Hohensinner, S., Habersack, H., Jungwirth, M., Zauner, G., 2004. Reconstruction of the
1178 characteristics of a natural alluvial river-floodplain system and hydromorphological changes
1179 following human modifications: the Danube River (1812-1991). River Res. Applic. 20, 25–41.
1180 https://doi.org/10.1002/rra.719

1181 Hudson, P.F., Middelkoop, H., Stouthamer, E., 2008. Flood management along the Lower
1182 Mississippi and Rhine Rivers (The Netherlands) and the continuum of geomorphic adjustment.
1183 Geomorphology 101, 209–236. https://doi.org/10.1016/j.geomorph.2008.07.001

1184 Ibisate, A., Díaz, E., Ollero, A., Acín, V., Granado, D., 2013. Channel response to multiple
1185 damming in a meandering river, middle and lower Aragón River (Spain). Hydrobiologia 712,
1186 5–23. https://doi.org/10.1007/s10750-013-1490-0

1187 Janssen, P., Stella, J.C., Räpple, B., Gruel, C.-R., Seignemartin, G., Pont, B., Dufour, S.,
1188 Piégay, H., 2021. Long-term river management legacies strongly alter riparian forest attributes
1189 and constrain restoration strategies along a large, multi-use river. Journal of Environmental
1190 Management 279, 111630. https://doi.org/10.1016/j.jenvman.2020.111630

1191 Kondolf, G.M., 1997. PROFILE: Hungry Water: Effects of Dams and Gravel Mining on River
1192 Channels. Environmental Management 21, 533–551. https://doi.org/10.1007/s002679900048

1193 Kondolf, G.M., Boulton, A.J., O'Daniel, S., Poole, G.C., Rahel, F.J., Stanley, E.H., Wohl, E.,
1194 Bång, A., Carlstrom, J., Cristoni, C., Huber, H., Koljonen, S., Louhi, P., Nakamura, K., 2006.
1195 Process-Based Ecological River Restoration: Visualizing Three-Dimensional Connectivity and
1196 Dynamic Vectors to Recover Lost Linkages. E&S 11, art5. https://doi.org/10.5751/ES-01747-
1197 110205

1198 Kroes, D.E., Hupp, C.R., 2010. The Effect of Channelization on Floodplain Sediment
1199 Deposition and Subsidence Along the Pocomoke River, Maryland. Journal of the American
1200 Water Resources Association 46, 686–699. https://doi.org/10.1111/j.1752-1688.2010.00440.x

1201 Lamouroux, N., Doutriaux, E., Terrier, C., Zylberblat, M., 1999. Modélisation des impacts de la
1202 gestion des débits réservés du Rhône sur les peuplements piscicoles. Bull. Fr. Pêche Piscic.
1203 45–61. https://doi.org/10.1051/kmae:1999020

1204 Liébault, F., Piégay, H., 2002. Causes of 20th century channel narrowing in mountain and
1205 piedmont rivers of southeastern France: causes of channel narrowing in SE France. Earth
1206 Surf. Process. Landforms 27, 425–444. https://doi.org/10.1002/esp.328

1207 Malanson, G.P., 1993. Riparian Landscapes, Cambridge Studies in Ecology. Cambridge
1208 University Press. https://doi.org/10.1017/CBO9780511565434

1209 McCoy, A.W., 2006. Numerical investigations using LES: exploring flow physics and mass
1210 exchange processes near groynes (Doctor of Philosophy). University of Iowa.
1211 https://doi.org/10.17077/etd.vt63cy20

1212 Morse, N.B., Pellissier, P.A., Cianciola, E.N., Brereton, R.L., Sullivan, M.M., Shonka, N.K.,
1213 Wheeler, T.B., McDowell, W.H., 2014. Novel ecosystems in the Anthropocene: a revision of
1214 the novel ecosystem concept for pragmatic applications. E&S 19, art12.
1215 https://doi.org/10.5751/ES-06192-190212

1216 Naiman, R.J., Décamps, H., 1997. The Ecology of Interfaces: Riparian Zones. Annu. Rev.
1217 Ecol. Syst. 28, 621–658. https://doi.org/10.1146/annurev.ecolsys.28.1.621

Nilsson, C., Berggren, K., 2000. Alterations of Riparian Ecosystems Caused by River Regulation. BioScience 50, 783. https://doi.org/10.1641/0006-3568(2000)050[0783:AORECB]2.0.CO;2

Olivier, J.-M., Carrel, G., Lamouroux, N., Dole-Olivier, M.-J., Malard, F., Bravard, J.-P., Piégay, H., Castella, E., Barthélemy, C., 2022. Chapter 7 - The Rhône River Basin, in: Tockner, K., Zarfl, C., Robinson, C.T. (Eds.), Rivers of Europe (Second Edition). Elsevier, pp. 391–451. https://doi.org/10.1016/B978-0-08-102612-0.00007-9

Papanicolaou, A.N., Fox, J.F., 2008. Investigation of Flow and Local Scour Characteristics around a Partially Submerged Permeable Barb, in: World Environmental and Water Resources Congress 2008. Presented at the World Environmental and Water Resources Congress 2008, American Society of Civil Engineers, Honolulu, Hawaii, United States, pp. 1–7. https://doi.org/10.1061/40976(316)254

Parrot, E., 2015. Analyse spatio-temporelle de la morphologie du chenal du Rhône du Léman à la Méditerranée. Lyon 3 University (Ph.D. Thesis).

Petts, G., 1984. Impounded Rivers. Wiley: Chichester.

Petts, G.E., 1987. Time-Scales for Ecological Change in Regulated Rivers, in: Craig, J.F., Kemper, J.B. (Eds.), Regulated Streams. Springer US, Boston, MA, pp. 257–266. https://doi.org/10.1007/978-1-4684-5392-8_17

Petts, G. E., Amoros, C., 1996. The fluvial hydrosystem, in: Petts, G.E., Amoros, C. (Eds.), The Fluvial Hydrosystems. Springer Netherlands, Dordrecht, pp. 1–12. https://doi.org/10.1007/978-94-009-1491-9_1

Petts, Geoffrey E., Amoros, C. (Eds.), 1996. Fluvial hydrosystems, 1st ed. ed. Chapman & Hall, London; New York.

Petts, G.E., Gurnell, A.M., 2005a. Dams and geomorphology: Research progress and future directions. Geomorphology 71, 27–47. https://doi.org/10.1016/j.geomorph.2004.02.015

Petts, G.E., Gurnell, A.M., 2005b. Dams and geomorphology: Research progress and future directions. Geomorphology 71, 27–47. https://doi.org/10.1016/j.geomorph.2004.02.015

Piégay, H., Bertrand, M., Räpple, B., Seignemartin, G., Parmentier, H., 2015. Analyse des processus de sédimentation dans le lit majeur et les annexes fluviales du RCC de Péage-de-Roussillon, Rapport final. Observatoire des sédiments du Rhône. Technical report.

Piégay, H., 2016. System approaches in fluvial geomorphology, in: Tools in Fluvial Geomorphology. John Wiley & Sons, Ltd, pp. 77–102. https://doi.org/10.1002/9781118648551.ch5

Piégay, H., Arnaud, F., Belletti, B., Bertrand, M., Bizzi, S., Carbonneau, P., Dufour, S., Liébault, F., Ruiz-Villanueva, V., Slater, L., 2020. Remotely sensed rivers in the Anthropocene: state of the art and prospects. Earth Surf. Process. Landforms 45, 157–188. https://doi.org/10.1002/esp.4787

Piégay, H., Hupp, C.R., Citterio, A., Dufour, S., Moulin, B., Walling, D.E., 2008. Spatial and temporal variability in sedimentation rates associated with cutoff channel infill deposits: Ain River, France. Water Resour. Res. 44. https://doi.org/10.1029/2006WR005260

Rahman, K., da Silva, A.G., Tejeda, E.M., Gobiet, A., Beniston, M., Lehmann, A., 2015. An independent and combined effect analysis of land use and climate change in the upper Rhone River watershed, Switzerland. Applied Geography 63, 264–272. https://doi.org/10.1016/j.apgeog.2015.06.021

Räpple, B., 2018. Sedimentation patterns and riparian vegetation characteristics in novel ecosystems on the Rhône River. Ecole Normale Supérieure de Lyon (Ph.D. Thesis).

Riquier, J., 2015. Réponses hydrosédimentaires de chenaux latéraux restaurés du Rhône français. Structures spatiales et dynamiques temporelles des patrons et des processus, pérennité et recommandations opérationnelles. Lyon 2 University (Ph.D. Thesis).

Riquier, J., Piégay, H., Lamouroux, N., Vaudor, L., 2017. Are restored side channels sustainable aquatic habitat features? Predicting the potential persistence of side channels as aquatic habitats based on their fine sedimentation dynamics. Geomorphology 295, 507–528. https://doi.org/10.1016/j.geomorph.2017.08.001

Riquier, J., Piégay, H., Šulc Michalková, M., 2015. Hydromorphological conditions in eighteen restored floodplain channels of a large river: linking patterns to processes. Freshw Biol 60, 1085–1103. https://doi.org/10.1111/fwb.12411

Risser, P.G., 1995. The Status of the Science Examining Ecotones. BioScience 45, 318–325. https://doi.org/10.2307/1312492

Savic, R., Ondrasek, G., Bezdan, A., Letic, L., Nikolic, V., 2013. Fluvial deposition in groyne fields of the middle course of the Danube River/Zasipanje medunaperskih polja (prostora izmedu regulacijskih pera) na srednjem toku Dunava. Tehnicki Vjesnik - Technical Gazette 20, 979+.

Schwartz, R., Kozerski, H.-P., 2003. Entry and Deposits of Suspended Particulate Matter in Groyne Fields of the Middle Elbe and its Ecological Relevance. Acta hydrochim. hydrobiol. 31, 391–399. https://doi.org/10.1002/aheh.200300496

Seignemartin, G., Riquier, J., Mourier, B., Winiarski, T., Piégay, H., 2022. Les marges alluviales endiguées du Rhône : trajectoires d'atterrissement, états des lieux hydro-sédimentaire et sanitaire, perspectives opérationnelles, in: Colloque SHF : « Aménagements et Biodiversité »,. Strasbourg, p. 10.

Seignemartin, G., 2020. Évolution contemporaine des « casiers Girardon » du Rhône : approche géohistorique à partir d'indicateurs morpho-sédimentaires, géochimiques et phytoécologiques. Lyon 2 University (Ph.D. Thesis).

1290 Simon, A., Rinaldi, M., 2006. Disturbance, stream incision, and channel evolution: The roles
1291 of excess transport capacity and boundary materials in controlling channel response.
1292 Geomorphology 79, 361–383. https://doi.org/10.1016/j.geomorph.2006.06.037

1293 Sukhodolov, A., Uijttewaal, W.S.J., Christof Engelhardt, 2002. On the correspondence
1294 between morphological and hydrodynamical patterns of groyne fields. Earth Surf. Process.
1295 Landforms 27, 289–305. https://doi.org/10.1002/esp.319

1296 Surian, N., 1999. Channel changes due to river regulation: the case of the Piave River, Italy.
1297 Earth Surf. Process. Landforms 24, 1135–1151. https://doi.org/10.1002/(SICI)1096-
1298 9837(199911)24:12<1135::AID-ESP40>3.0.CO;2-F

1299 Surian, N., Rinaldi, M., 2003. Morphological response to river engineering and management
1300 in alluvial channels in Italy. Geomorphology 50, 307–326. https://doi.org/10.1016/S0169-
1301 555X(02)00219-2

1302 Tena, A., Piégay, H., Seignemartin, G., Barra, A., Berger, J.F., Mourier, B., Winiarski, T., 2020.
1303 Cumulative effects of channel correction and regulation on floodplain terrestrialization patterns
1304 and connectivity. Geomorphology 354, 107034.
1305 https://doi.org/10.1016/j.geomorph.2020.107034

1306 Thorel, M., Piégay, H., Barthelemy, C., Räpple, B., Gruel, C.-R., Marmonier, P., Winiarski, T.,
1307 Bedell, J.-P., Arnaud, F., Roux, G., Stella, J.C., Seignemartin, G., Tena-Pagan, A.,
1308 Wawrzyniak, V., Roux-Michollet, D., Oursel, B., Fayolle, S., Bertrand, C., Franquet, E., 2018.
1309 Socio-environmental implications of process-based restoration strategies in large rivers:
1310 should we remove novel ecosystems along the Rhône (France)? Reg Environ Change 18,
1311 2019–2031. https://doi.org/10.1007/s10113-018-1325-7

1312 Tockner, K., Stanford, J.A., 2002a. Riverine flood plains: present state and future trends. Envir.
1313 Conserv. 29, 308–330. https://doi.org/10.1017/S037689290200022X

Tockner, K., Stanford, J.A., 2002b. Riverine flood plains: present state and future trends. Envir. Conserv. 29, 308–330. https://doi.org/10.1017/S037689290200022X

Vauclin, S., Mourier, B., Tena, A., Piégay, H., Winiarski, T., 2020. Effects of river infrastructures on the floodplain sedimentary environment in the Rhône River. J Soils Sediments 20, 2697–2708. https://doi.org/10.1007/s11368-019-02449-6

Vázquez-Tarrío, D., Tal, M., Camenen, B., Piégay, H., 2019. Effects of continuous embankments and successive run-of-the-river dams on bedload transport capacities along the Rhône River, France. Science of The Total Environment 658, 1375–1389. https://doi.org/10.1016/j.scitotenv.2018.12.109

Ward, J.V., 1998. Riverine landscapes: Biodiversity patterns, disturbance regimes, and aquatic conservation. Biological Conservation 83, 269–278. https://doi.org/10.1016/S0006-3207(97)00083-9

Ward, J.V., Tockner, K., Schiemer, F., 1999. Biodiversity of floodplain river ecosystems: ecotones and connectivity1. Regul. Rivers: Res. Mgmt. 15, 125–139. https://doi.org/10.1002/(SICI)1099-1646(199901/06)15:1/3<125::AID-RRR523>3.0.CO;2-E

Winterbottom, S.J., 2000. Medium and short-term channel planform changes on the Rivers Tay and Tummel, Scotland. Geomorphology 34, 195–208. https://doi.org/10.1016/S0169-555X(00)00007-6

Wyżga, B., 2001. A Geomorphologist's Criticism of the Engineering Approach to Channelization of Gravel-Bed Rivers: Case Study of the Raba River, Polish Carpathians. Environmental Management 28, 341–358. https://doi.org/10.1007/s0026702454

Zawiejska, J., Wyżga, B., 2010. Twentieth-century channel change on the Dunajec River, southern Poland: Patterns, causes and controls. Geomorphology 117, 234–246. https://doi.org/10.1016/j.geomorph.2009.01.014

9. Supplementary material

Annex 1: engineering interventions (phase 1 and 2) and associated features on the Rhône River

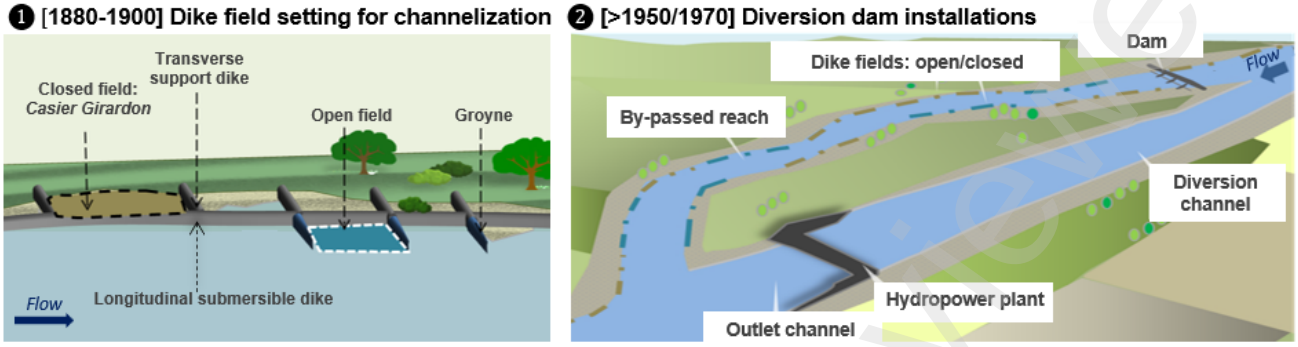

Annex 2: characteristics of the photograph series

Year	Source	Date	Scale or resolution*	Photo type	Color type	Mean discharge (m^3/s) **	Mission ID
1938	IGN	17/08/1938	1/24172	Argentic	B&W	877	C3410-0221_1938
1949	IGN	01/10/1949	1/16673	Argentic	B&W	342	C3031-0551_1949
1974	IGN	26/07/1974	1/18577	Argentic	B&W	510	C3033-0201_1974
1979	IGN	20/06/1979	1/17515	Argentic	B&W	1140	C2934-0041_1979
1982	IGN	09/07/1982	1/14202	Argentic	B&W	810	C3329-0031_1982
1986	IGN	25/06/1986	1/20718	Argentic	Color	882	C2928-0012_1986
1991	IGN	16/07/1991	1/17665	Argentic	Color	731	C91SAA2002_1991
2002	IGN	20/05/2002	1/25306	Argentic	Color	1200	CP02000012_2002
2009	IGN	04/06/2009	66 cm	Numeric	Color	634	CP09000262_FD38F80

*the scale varies slightly from one shot to another in the same campaign

**mean discharge levels at Ternay gauging station – non-bypassed part